Secular changes in the importance of neritic carbonate deposition as a control on the magnitude and stability of Neoproterozoic ice ages

Andy Ridgwell and Martin Kennedy

Department of Earth Sciences, University of California - Riverside, Riverside, California, USA.

We hypothesize that secular evolution in the control of calcium carbonate deposition dictated the severity of Neoproterozoic ice ages. In the modern ocean, reduction in carbonate deposition on the continental shelves can be compensated for by the increased preservation in deep sea sediments of biogenic carbonate originating from planktic calcifiers living in the open ocean. The result is that ocean carbonate chemistry is strongly buffered and the carbon-climate system relatively stable. However, before the advent of metazoan biomineralization in the Cambrian and proliferation of calcareous plankton during the Mesozoic, carbonate deposition would have been largely restricted to shallow water photic environments in the Neoproterozoic. A fall in sea level acting to restrict the photosynthetic area within Precambrian seas would necessarily initially decrease the global rate of carbonate deposition without being compensated by the typical Phanerozoic deep sea sedimentary 'buffer'. Ultimately, carbonate precipitation would reestablish itself at a greater local rate throughout the more areally restricted seas. The resulting higher degree of ocean saturation translates to substantially lower atmospheric CO_2 and colder terrestrial conditions. Ice ages of near-global extent and multi million-year duration can thus be understood as a direct consequence of the weak 'buffering' of the Precambrian carbon cycle, amplified by feedbacks involving CO_2 and climate. Both the widespread occurrence and observed thickness of 'cap' (dolostone) carbonate deposited during post-glacial flooding of the shelves are explicit predictions of this hypothesis, and record the rapid removal from a highly oversaturated ocean of excess alkalinity accumulated during the glacial.

1. INTRODUCTION

The close timing of the first appearance of multicellular organisms [*Runnegar*, 2000] with the last of what were likely the most severe ice ages of Earth history [*Crowell et al.*, 1999] raises the obvious question of causality. Phenomena associated with these ice ages imply an extremity of climate unmatched by the Phanerozoic record and include; (i) grounded ice sheets at equatorial paleolatitudes [*Evans*, 2000; *Sohl et al.*, 1999], (ii) high magnitude variations in the carbon isotope (carbonate $\delta^{13}C$) record (+10 to -6‰ PDB) [*Hoffman et al.*, 1998; *Jacobsen and Kaufman*, 1999; *Kennedy et al.*, 1998], and (iii) ubiquitous precipitation of a thin layer of carbonate (known as "cap carbonate") directly overlying glacial deposits [*Williams*, 1979; *Hoffman and Schrag*, 2002; *James et al.*, 2001; *Kennedy*, 1996; *Kennedy et al.*, 1998, 2001a,b; *Myrow and Kaufman*, 1999]. In the controversial 'snowball Earth' hypothesis [*Hoffman et al.*, 1998; *Hoffman and Schrag*, 2002], the severe perturbation to the global carbon cycle implied by these physical features is taken as evidence for a prolonged period of surface ocean freezing (ca. 10 Ma), which extinguishes marine ecosystems and provides an 'evolutionary bottleneck', ultimately driving the proliferation of Metazoa. While changes in the biosphere are likely to have important evolutionary influences on life, it is also apparent that life can strongly affect the biosphere. Here we adopt a different strategy for understanding these anomalous Neoproterozoic glacial phenomena by identifying the first order difference between Phanerozoic and Precambrian carbon cycling that arises with the addition of carbonate depositional controls imparted by carbonate secretion bio-innovation. Through this approach, we find that the phenomena present in the Neoproterozoic record are predictable consequences of a less highly 'evolved' global carbon cycle.

2. HARD 'SNOWBALL' OR SOFT 'SLUSHBALL EARTH'?

2.1 The 'Snowball'

In an attempt to make sense of the variety of both physical and geochemical data available from the Precambrian geological record, *Kirschivink* [1992] proposed the occurrence of a 'snowball Earth'. He envisaged the Earth entering a completely frozen state several times during the late Neoproterozoic (although the exact number of distinct glacial episodes is still controversial [*Kennedy et al.*, 1998]); a state terminated once out-gassed mantle CO_2 accumulating in the atmosphere became sufficient to warm the Earth and melt the ice cover. These ideas were subsequently extended to consider certain aspects of the carbonate $\delta^{13}C$ record and the enigmatic presence of the 'cap' carbonates, the latter being explained as a consequence of greatly enhanced silicate rock weathering rates in an intense 'greenhouse' climate immediately following ice melt-back [*Hoffman et al.*, 1998].

Underpinning this thesis is an 'ice-albedo' feedback instability in the Earth system [*Hoffman et al.*, 1998; *Hoffman and Schrag*, 2002], the theoretical existence of which was originally predicted by early energy balance climate models [*Budyko*, 1969; *Cahalan and North*, 1979]. The climatic instability is triggered by the extension of sea ice to some critical latitude; perhaps lying ±30° from the Equator [*Caldeira and Kasting*, 1992]. Any further cooling of climate then initiates a runaway chain of events involving sea ice expansion and further cooling (the 'ice-albedo' feedback [*Budyko*, 1969]), until sea ice reaches the Equator [*Caldeira and Kasting*, 1992] and the ocean is everywhere covered in (sea) ice. The existence of a reflective ice cover results in highly inefficient capture of solar energy and an extreme cooling of the Earth's surface [*Caldeira and Kast-*

ing, 1992]. For the system to exit this state, a very substantial radiative forcing of climate is required in order to warm the Equator sufficiently to start melting back the sea ice. One possible means of achieving this forcing could arise should no weathering of silicate rock take place on the frozen planet. Without any means of removal by weathering reactions, CO_2 originating from volcanic and metamorphic sources would gradually accumulate in the atmosphere. When the partial pressure of CO_2 reaches ca. 0.12 bar, the trapping of outgoing infra-red radiation would result in a surface warming (via the 'Greenhouse effect') sufficient to make the equatorial ice line unstable [*Caldeira and Kasting*, 1992]. The albedo feedback then operates in reverse, the ice melts rapidly and the glacial ends. The time scale for this slow warming process to be completed could be as long as 30 Ma [*Caldeira and Kasting*, 1992]. *The 'snowball Earth' hypothesis thus accounts for the inferred multi-million year duration of the glacial event in terms of the length of time required to buildup the required excess CO_2 in the atmosphere and exit from the ice-albedo feedback instability* [*Hoffman et al.*, 1998; *Hoffman and Schrag*, 2002].

The sea ice instability required by the snowball Earth hypothesis has been demonstrated in a number of GCM and coupled climate-ice sheet models [*Baum and Crowley*, 2001; *Crowley et al.*, 2001; *Donnadieu et al.*, 2003; *Hyde et al.*, 2000; *Jenkins and Smith*, 1999]. However, the use of a fixed depth mixed layer ('slab') representation of the ocean in all these models cautions against drawing firm conclusions regarding whether an ice-albedo instability exists in the real Earth system [*Jenkins and Smith*, 1999; *Poulsen*, 2003]. In contrast, atmospheric GCM models coupled either to a deeper seasonal mixed layer ocean [*Chandler and Sohl*, 2000] or a full ocean GCM [*Poulsen et al.*, 2001, 2002; *Poulsen*, 2003] have conspicuously failed to find any evidence for an ice-albedo instability, regardless of how 'favorably' the initial conditions are set [*Poulsen*, 2003]. Re-analysis with coupled models in which both oceanic and atmospheric meridional energy transports are separately resolved indicates that the strength of the (sea) ice-albedo feedback is much weaker than earlier idealized models suggested [*Bendtsen*, 2002]. This questions the underpinning assumption of *Kirschivink* [1992] and *Hoffman et al.* [1998]. Because the viability of a 'snowball Earth' state rests fundamentally on the existence and latitudinal limits of sea-ice instability, further work with particular focus on fully-resolved coupled ocean-atmosphere models is essential for the further support or falsification of this hypothesis.

2.2 The 'Slushball'

A climate state characterized by the equilibrium co-existence of Equatorial ice sheets with an open tropical ocean is consistent with geological evidence for low latitude glaciation and represents an alternative interpretation to an entirely ice-covered 'hard snowball' world. This 'open water' climatic solution (dubbed 'slushball Earth') is also predicted by coupled climate-ice sheet models [*Baum and Crowley*, 2001; *Crowley et al.*, 2001; *Hyde et al.*, 2000]. However, this interpretation does offer certain advantages over the 'snowball Earth'. For instance, the widespread occurrence of cyclic Ice Rafted Debris (IRD) rich and IRD-absent diamictite layers are suggestive of periodic and widespread surges of an ice sheet into the open ocean [*Condon et al.*, 2002] and may be analogous to the generation of Heinrich layers in the North Atlantic during the late Quaternary [*Heinrich*, 1988]. Similarly, Neoproterozoic age glaciogenic sedimentary rocks of the Ghadir Manqil Formation, Oman, have been interpreted as recording cycles of relative sea-level change and of strongly pulsed glacial advance and retreat [*Leather et al.*, 2002]. These geological observations appear to be at odds with a completely frozen surface ocean. In general, evidence of an active cryosphere and hydrological cycle during the glaciation [*Arnaud and Elyes*, 2002; *Condon et al.*, 2002; *Leather et al.*, 2002; *McMechan*, 2000] is more easily reconcilable with the presence of a substantial area of open water to act as a moisture source.

Furthermore, the open water solution requires only moderate changes in atmospheric CO_2 to terminate glacial conditions [*Crowley et al.*, 2001]. It is also easier to understand the persistence of viable life through the glacial if the ocean surface is not entirely ice-covered. In the 'slushball', an equatorial belt of open water provides a refugium for multicellular life [*Hyde et al.*, 2000, 2001; *Runnegar*, 2000].

Despite these advantages, the open water solution has been dismissed by the proponents of the 'snowball Earth' hypothesis. Two primary grounds for rejection have been advanced; (i) glacial longevity – it is argued that only a 'snowball Earth', locked in a frozen state is inherently long-lived. An ice-free equatorial ocean, with "ice fronts [that] miraculously approach but never cross the ice-albedo instability threshold" [*Hoffman and Schrag*, 2002] could not be stable [*Hoffman*, 2000; *Hoffman and Schrag*, 2002; *Schrag and Hoffman*, 2001], and (ii) 'cap' carbonate occurrence – the snowball Earth hypothesis posits extremely rapid weathering following deglaciation to provide the necessary alkalinity. This was originally envisaged as being the weathering of silicate rocks [*Hoffman et al.*, 1998], but more recently assumes a two-stage process with a transition from a dominance of carbonate to silicate rock weathering [*Higgins and Schrag*, 2003]. In contrast, the 'slushball' has no inherent mechanism to explain the occurrence of the 'cap' carbonate layers [*Hoffman and Schrag*, 2002; *Schrag and Hoffman*, 2001].

Here we identify a first order difference between Precambrian and modern carbon cycles which explains the extremity of Neoproterozoic glaciation: the absence of a well-developed deep-sea carbonate sink prior to the proliferation of calcareous plankton in the Phanerozoic. This leads us to a geochemical model [*Ridgwell et al.*, 2003b] that supports a 'slushball' interpretation of glacial climate. The model predicts both extensive and long-lived glaciation, as well as the timing of the alkalinity flux recorded by the 'cap' carbonate.

3. CARBONATE DEPOSITIONAL CONTROL OF NEOPROTEROZOIC ICE AGES – A NEW HYPOTHESIS

3.1 Modern Carbon Cycling

A key component of the global carbon cycle throughout Earth history has been the cycling of calcium carbonate ($CaCO_3$). Today, biogenic precipitation of $CaCO_3$ in the open ocean dominates the marine carbonate budget [*Milliman*, 1993; *Milliman and Droxler*, 1996]. This, in turn, is dominated by the calcification activity of planktic foraminifers and coccolithophores [*Schiebel*, 2002]. Although more than 80% of carbonate precipitated in the open ocean dissolves either in the water column or within the uppermost sediment layers, accumulation of $CaCO_3$ in deep sea sediments still represents around half of the present-day global burial rate of $CaCO_3$, with the remainder accumulating in shallow water environments [*Milliman and Droxler*, 1996].

The importance of the deep sea sedimentary $CaCO_3$ sink lies in the fundamental role it plays in stabilization of the concentration of CO_2 in the atmosphere. This works as follows. Any change in the dissolved inorganic carbon (DIC = $CO_{2(aq)}$ + HCO_3^- + CO_3^{2-}) inventory or *p*H of the ocean will affect the amount of DIC in the form of carbonate ions (CO_3^{2-}) [*Zeebe and Wolf-Gladrow*, 2001]. The stability of the calcium carbonate crystal structure, represented by the saturation state (also known as the solubility ratio) Ω, is directly related to the ambient concentration of CO_3^{2-}; $\Omega = [Ca^{2+}]\times[CO_3^{2-}]/K_{sp}$, where K_{sp} a solubility constant [*Zeebe and Wolf-Gladrow*, 2001]. As a result, the dissolution of $CaCO_3$ in deep sea sediments will respond to changes in ocean carbonate saturation. Furthermore, because the removal rate of CO_3^{2-} is positively correlated with $[CO_3^{2-}]$, the response is of the form of a negative (stabilizing) feedback. For instance, higher $[CO_3^{2-}]$ will equate to increased $CaCO_3$ stability and $CaCO_3$ burial rate, which in turn equates to a higher removal rate of CO_3^{2-} from the ocean. This provides a restoring forcing of $[CO_3^{2-}]$ back towards the original equilibrium value. (This feedback works similarly on an initial lowering of $[CO_3^{2-}]$.) Modern ocean carbonate chemistry is thus 'buffered' against perturbation.

Of particular relevance to ice ages is a carbon cycling phenomenon that arises because the Earth's surface area is not uniformly distributed with elevation, and has gently sloping continental shelves giving way to relatively steeper slopes at greater depth (Figure 1). In the modern system, a fall in sea level will restrict the area available for coral reef growth and other forms of shallow water carbonate deposition, reducing $CaCO_3$ accumulation rates and driving higher ocean [CO_3^{2-}]. This will shift the aqueous carbonate equilibrium, $CO_2 + CO_3^{2-} + H_2O \leftrightarrow 2HCO_3^-$ to the right and drive atmospheric CO_2 lower [*Zeebe and Wolf-Gladrow*, 2001]. This is the basis for the 'coral reef' hypothesis for the control of CO_2 over the glacial-interglacial cycles of the late Quaternary [*Berger*, 1982; *Munhoven and François*, 1996; *Opdyke and Walker*, 1992; *Ridgwell et al.*, 2003a; *Walker and Opdyke*, 1995] (Figure 2). This reduction in neritic carbonate deposition is, however, largely compensated for by the enhanced preservation in deep sea sediments of calcium carbonate produced by pelagic calcifiers and a lowering of the lysocline. This compensation or buffering mechanism limits the atmospheric response to changes in sea level during the Quaternary to ca. 20-40 ppmv [*Ridgwell et al.*, 2003a].

3.2 Neoproterozoic Carbon Cycling

Without a pelagic carbonate flux to the deep ocean, the situation in the Precambrian is fundamentally different, and the importance of a 'coral reef' effect substantially greater. Prior to the advent of metazoan biomineralization around the time of the Precambrian-Cambrian boundary [*Wood et al.*, 2002], and in particular, the proliferation of coccolithophores and foraminifera in the Mesozoic [*Boss and Wilkinson*, 1991], carbonate deposition would have been largely restricted to the photic zone (Figure 3). The dominance of neritic depositional environments at this time is supported by the observed composition of ophiolite suites, which indicate disproportionately less pelagic carbonate accumulating in deep sea sediments before ca. 300 Ma [*Boss and Wilkinson*, 1991]. With neritic carbonate deposition the dominant mechanism of CO_3^{2-} removal, it follows that atmospheric CO_2 would have been much more sensitive to sea level change; especially in cases where sea level falls below the shelf slope break. It is this increased sensitivity of CO_2 that is the key to understanding the extremity of Neoproterozoic ice ages.

In the modern system with its deep sea 'buffer', imbalances induced between CO_3^{2-} inputs (rock weathering) and outputs ($CaCO_3$ deposition) by a change in the area of shallow water depositional environments is primarily corrected by a preservational response of carbonate in deep sea sediments (although there is also a component of pelagic calcification response to ambient surface ocean CO_3^{2-} in the modern system [*Barker and Elderfield*, 2002; *Riebesell et al.*, 2000]). In the Precambrian, it is an increase in the rate of neritic carbonate precipitation in a commensurately smaller area that must restore the balance to restore steady state. The precipitation of carbonate minerals occurs at a rate dependent on ambient saturation, typically taking the form of a proportionality with $(\Omega\text{-}1)^n$ [*Zhong and Mucci*, 1993], where n is a measure of how strongly $CaCO_3$ precipitation rate responds to a change in $[CO_3^{2-}]$. The result of this is that with rising oceanic super-saturation following a fall in sea level, increasing precipitation rates per unit area will eventually be able to compensate for the smaller photic area available for deposition. The parameter n determines how strongly neritic $CaCO_3$ deposition responds to a perturbation of sea level, and thus how effectively ocean saturation state and atmospheric CO_2 is 'buffered'. For instance, a low value of n will require a large increase in Ω to alter the precipitation rate sufficiently to reestablish equilibrium of sources and sinks of CO_3^{2-}. The result of this will be a substantial drawdown in atmospheric CO_2. An analogous situation has been analyzed previously with respect to an extinction-driven reduction in pelagic carbonate productivity at the Cretaceous/Tertiary boundary [*Caldeira and Rampino*, 1993].

Below, we explore the dynamics of the Neoproterozoic carbon cycle and the sensitivity of atmospheric CO_2 to sea level variation and test whether secular changes in the importance of neritic carbonate depositional controls can explain the magnitude and stability of Neoproterozoic ice. We employ a numerical model for this analysis [*Ridgwell et al.*, 2003b]. This calculates the change in ocean carbonate saturation and atmospheric CO_2 that would arise from a reduction in the area available for (neritic) carbonate deposition.

4. A MODEL FOR NEOPROTEROZOIC CO_2

4.1 Model Description

Analysis of the global carbon cycle on timescales relevant to Neoproterozoic glaciation requires model integration for >1 Myr. In contrast, air-sea gas exchange processes which link ocean and atmospheric carbon reservoirs require a time step of order months for numerical stability of the model. Use of a relatively spatially unresolved model is therefore essential. Our chosen strategy is based on the 'PANDORA' atmosphere-ocean carbon cycle 'box' model of *Broecker and Peng* [1986]. The ocean is coupled to a representation of the preservation and burial of $CaCO_3$ in deep sea sediments, following *Ridgwell* [2001] and *Ridgwell et al.* [2002]. The overall atmosphere-ocean-sediment scheme is similar to established modeling tools such as devised by *Caldeira and Rampino* [1993], *Munhoven and François* [1996], and *Walker and Opdyke* [1995].

Loss of dissolved inorganic carbon (DIC) and alkalinity (ALK) from the ocean due to sedimentary burial of $CaCO_3$ is balanced by prescribing DIC and ALK fluxes following *Walker and Opdyke* [1995], but omitting terms representing the erosion (and formation) of sedimentary kerogen. Long-term (order >10^5 yr) stabilizing feedback on the system is provided by modifying the DIC (15 Tmol yr^{-1}) and ALK (40 Tmol eq yr^{-1}) fluxes arising from terrigeneous silicate and carbonate rock weathering according to the pre-vascular plant formulation of the GEOCARB model [*Berner*, 1990]. The rate of volcanic CO_2 out-gassing (5 Tmol yr^{-1} [*Walker and Opdyke*, 1995]) is left constant. We impose no additional reduction in global weathering rates explicitly associated with an increase in terrestrial ice cover, consistent with analyses of the late Quaternary glacial geochemical system which indicate little difference in solute fluxes between glacial and interglacial times [*Gibbs and Kump*, 1994; *Jones et al.*, 2002; *Munhoven*, 2002].

An idealized representation of shallow water carbonate buildup is formulated based on the arguments outlined earlier, and coupled to the surface ocean. Because primary precipitation of $CaCO_3$ during the Neoproterozoic is dominantly associated with phototrophic (mainly cyanobacterial) communities [*Riding*, 2000], we assume deposition to be restricted to the photic zone, which is taken to be the uppermost sunlit 100 m. The strength of the $CaCO_3$ sink is then proportional to the total neritic area, A (found by integrating the Earth's surface area flooded to a depth of 100 m or less), to give; $A \times k \times (\Omega -1)^n$. This treatment is comparable to previous schemes that have been devised for Phanerozoic shallow water carbonate deposition [*Caldeira and Rampino*, 1993; *Munhoven and François*, 1996]. The value of the precipitation rate scaling constant, k is constrained by the requirement that the system should initially be at steady state, with weathering and riverine input balancing the global (neritic) deposition rate of $CaCO_3$. The appropriate value of n for the Precambrian environment is less easy to constrain. At one extreme, abiotic precipitation of calcite exhibits a highly non-linear response to ambient saturation with n in the range $1.9 \leq n \leq 2.8$ at 25°C [*Zhong and Mucci*, 1993]. A small change in $[CO_3^{2-}]$ then has a disproportionately large influence on precipitation rate. In contrast, modern biological systems such as individual corals and whole reef communities appear to be considerably less sensitive, with an approximately first order dependence on Ω [*Leclercq et al.*, 2000; *Marshall and Clode*, 2002]. Additional complications arise because the value of n also varies with other variables such as temperature [*Burton and Walter*, 1987] (which gives neritic deposition an apparent latitudinal dependence [*Opdyke and Wilkinson*, 1993]), ionic strength [*Zuddas and Mucci*, 1998], CO_2 partial pressure [*Zuddas and Mucci*, 1994], and the presence of dissolved inorganic matter [*Lebrón and Suárez*, 1996, 1998]. We therefore initially follow previous (Phanerozoic) carbon cycling studies and assume a uniform value of n = 1.7 [*Caldeira and Rampino*, 1993; *Munhoven and François*, 1996]. However, we will later explore the implications of alternative dependencies.

4.2 Initial Conditions

The carbon cycle is configured for the Precambrian as follows. The absence of planktic calcifiers is achieved by setting the export flux ratio of $CaCO_3$ to particulate organic carbon (POC) in the PANDORA ocean carbon cycle model to zero. Ocean chemistry is determined consistent with two criteria; (i) surface ocean in equilibrium with a mixing ratio of CO_2 in the atmosphere of 3400 ppmv. This is a value that has been demonstrated to be sufficient to prevent the formation of ice sheets in climate models of the Neoproterozoic including the effects of a weaker Sun [*Crowley et al.*, 2001; *Hyde et al.*, 2000; *Jenkins and Smith*, 1999], and (ii) mean ocean mixed layer saturation state (calculated with respect to aragonite) of Ω_0 = 6.5, which is consistent with a Neoproterozoic ocean more highly saturated than at present [*Grotzinger and James*, 2000; *Grotzinger and Knoll*, 1995; *James et al.*, 2001]. Ocean DIC and ALK are then uniquely determined if assumptions are made about [Ca^{2+}], for which a present-day value of 10 mmol kg^{-1} is adopted. Mean ocean DIC and ALK are then; 9.494 mmol kg^{-1} and 9.526 mmol eq kg^{-1}, respectively. We note that analysis of the ambient and micro- geochemical conditions that lead to the calcification of cyanobacteria [*Arp et al.*, 2001] suggests the absence of calcified microbes under our chosen initial conditions, despite the highly super-saturated state of the ocean. This is in agreement with geologic observations of the general absence of calcified microbes in carbonates of this period [*Arp et al.*, 2001; *Riding*, 2000].

An alternative model configuration with a modern mode of carbonate deposition is formulated to highlight the importance of abundant planktic calcification and associated existence of a responsive deep sea sedimentary buffer in stabilizing CO_2. In this the $CaCO_3$:POC ratio is set to 0.2, and ocean chemistry determined to achieve an atmospheric CO_2 concentration of 3400 ppmv as before. However, the values of Ω_0 (3.1) and k are now set to achieve a 50:50 partitioning of $CaCO_3$ accumulation between neritic and deep sea sedimentary sinks [*Milliman*, 1993] and an inter-basin distribution of $CaCO_3$ consistent with the modern system. Initial DIC and ALK are then determined as; 6.546 mmol kg^{-1} and 6.445 mmol eq kg^{-1}, respectively (again with present-day [Ca^{2+}]).

4.3 Methodology

To explore the importance of carbonate depositional controls on CO_2 stability, we perturb available neritic depositional area by prescribing a reduction in sea level in the carbon cycle model. This is done to simulate the effect of glacial inception and the early stages of ice sheet growth. The prescribed 100 m magnitude of sea level fall corresponds to the growth of an ice sheet of volume comparable to that characterizing the late Quaternary. Assuming modern topography [*ETOPO5*, 1988] this results in ~3.2-fold reduction in neritic area (Figure 1). This loss in neritic depositional area induces an imbalance between the sources and sinks of CO_3^{2-}. Ocean carbonate chemistry departs from its initial conditions, and the saturation state of the surface ocean (Ω_{arg}) increases. This continues until carbonate precipitation rates are sufficiently high to counter the reduced neritic area and balance is reestablished between the sources and sinks of CO_3^{2-}. The response of atmospheric CO_2 to this change in ocean saturation state is recorded. This sequence of events is shown schematically in Figure 4.

5. SENSITIVITY OF CO_2 TO INCIPIENT GLACIATION

5.1 Atmospheric CO_2 Response to Sea Level Fall

The Precambrian carbon cycle exhibits a high degree of CO_2 sensitivity to incipient glaciation and sea level fall (Figure 5). In the absence of planktic calcifiers, atmospheric CO_2 responds sharply, reaching a minimum of 2214 ppmv within about 100 kyr. This represents a 2.3 W m^{-2} reduction in the radiative forcing of the climate system; a value equal in magnitude (but opposite in sign) to the total anthropogenic 'greenhouse gas' forcing at present [*Ramaswamy et al.*, 2001]. In contrast, with abundant biogenic calcification in the surface waters of the open ocean CO_2 falls only to 3168 ppmv, a response just under one fifth as great as exhibited by the Precambrian system. Thus, as expected, any reduction in the neritic sink in the modern system is efficiently compensated for by increased carbonate preservation and burial in deep-sea sediments. In both cases lower CO_2 results in reduced rates of silicate weathering [*Berner*, 1990], driving an excess of mantle and metamorphic CO_2 input to the system over its removal. This imbalance acts to curtail the magnitude of the CO_2 minimum that can be achieved and subsequently drives the system back towards its initial state (CO_2 = 3400 ppmv).

Thus far, we have assumed modern topography. However, the existence of extensive rifted, subsiding margin, and intracratonic shallow water environments in the late Neoproterozoic (e.g., *Arnaud and Elyes* [2002], *James et al.* [2001], *Leather et al.* [2002], *Prave* [2002]) would result in a proportionally greater reduction in neritic area occurring with a fall in sea level (Figure 3). To assess the sensitivity of CO_2 in a system with a greater shelf-to-slope contrast we modify the modern hypsographic profile by increasing the area lying above the shelf break by a factor of three (Figure 1). This gives a total initial area of shallow water (neritic) environments of 6.1×10^{13} m^2, equivalent to just over one third of present-day cratonic area, but still less than is believed to have occurred during the Paleozoic when high sea level stands resulted in typical flooding extents of between 17 and 88% of total continental area [*Algeo and Selavinsky*, 1995]. The model is re-run and forced with the same 100 m magnitude perturbation of sea level as before. Now, the enhancement of the initial neritic area results in a 10-fold reduction in area with sea level fall. The concentration of CO_2 in the atmosphere is predicted as before.

In assessing the CO_2 response, we considered a range of possible assumptions regarding how strongly $CaCO_3$ precipitation rate responds to a change in ambient $[CO_3^{2-}]$; n = 1.0 (modern coral-like response [*Leclercq et al.*, 2000; *Marshall and Clode*, 2002]), n = 1.7 (the baseline case, following *Caldeira and Rampino* [1993] and *Munhoven and François* [1996]), and n = 2.5 (a more 'abiotic' mode of precipitation [*Zhong and Mucci*, 1993]). Depending on the value of the model parameter n, atmospheric CO_2 now attains a minimum as low as 859 ppmv (with n = 1.0), before the silicate weathering feedback starts to drive the system back towards initial conditions as before (Figure 6). However, the system is less susceptible to perturbation in the abiotic case (n = 2.5), and produces a less pronounced CO_2 minimum of 1820 ppmv. The corresponding reduction in radiative forcing of climate due to reduced CO_2 falls between 3.3 and 7.3 W m^{-2}.

It should be noted that the details of the atmosphere-ocean-sediment carbon cycle model used are not critical to our conclusions, and a comparable response to 10-fold reduction in neritic area is exhibited by the model of *Caldeira and Rampino* [1993] [*Caldeira*, pers com]. The assumption that prescribed sea level change takes place near instantaneously (within 1 kyr) appears to be similarly unimportant. We have tested the effect of sea level changing linearly over a period of 10 kyr, and found virtually no difference in CO_2 response. In contrast, the predicted atmospheric CO_2 minimum is highly dependent on the assumed initial value which we take to be 3400 ppmv in the baseline scenario. The results of sensitivity analysis of this dependence are shown in Figure 7. Because the magnitude of the CO_2 draw-down attained is approximately in proportion to the initial CO_2 value, the associated degree of radiative cooling is not strongly dependent on the assumed value of initial atmospheric CO_2. The *climatic* (surface cooling) importance of our mechanism is therefore independent of the assumed initial (atmospheric CO_2) conditions.

5.2 CO_2 Response Limitation by Pelagic Precipitation

An important caveat to our results concerns the possibility that significant pelagic carbonate precipitation takes place as the ocean becomes increasingly supersaturated, perhaps analogous to the occurrence of present-day 'whiting' events [*Robbins et al.*, 1997]. Precipitation of carbonate in the open ocean has the potential to limit the maximum drawdown in atmospheric CO_2 possible due to a fall in sea level. This is because it creates an additional sedimentary sink of $CaCO_3$. The difficulty in quantifying this process is in determining what the likely saturation threshold might be for pelagic carbonate precipitation to come to dominate the global mass budget. The marine geochemical conditions under which whitings occur in the modern ocean is controversial. One explanation for whitings in the Bahama Banks is biologically-induced or inorganic-physiochemical spontaneous precipitation of aragonite crystals in the water column [*Robbins and Blackwelder*, 1992; *Robbins et al.*, 1997]. If correct, the relatively low degree of super-saturation of these waters with Ω_{arg} typically lying between 1.95 and 3.5 would tend to suggest that whitings could be pervasive in the more highly supersaturated Neoproterozoic ocean. However, the balance of evidence strongly suggests that the Bahaman whitings are primarily a re-suspension of underlying sedimentary material [*Broecker et al.*, 2000; *Boss and Neumann*, 1993; *Morse et al.*, 2003]. Observations made in lake and other hydro-chemically restricted environments suggest only minor biologically-induced benthic precipitation (with no evidence of pelagic precipitation) when $7 \leq \Omega_{arg} \leq 11$ [*Arp et al.*, 1999, 2003]. Experimentally, spontaneous (homogeneous) nucleation in sea water solutions is not observed until values of Ω_{cal} > ~20 - 25 [*Morse and He*, 1993]. It is only in extreme chemical environments, such the mixing zones surrounding particular thermal springs (at a theoretical 100-fold super-saturation) do apparently inorganic-physiochemical 'whitings' occur [*Arp et al.*, 1999].

Clearly, the uncertainties associated with pelagic precipitation are substantial. However, based on these arguments it would seem that biologically-induced precipitation of $CaCO_3$ in the Neoproterozoic open ocean is highly unlikely for $\Omega_{arg} < 10$. Inorganic-physiochemical precipitation could ultimately dominate the global budget, but probably only for supersaturation $\Omega_{arg} > 20$.

We illustrate the potential role of pelagic carbonate precipitation in modifying system behavior by means of a sensitivity analysis (Figure 8). In this test, we create an additional sink of $CaCO_3$ that removes all 'excess' CO_3^{2-} from each surface ocean 'box' in the model whenever the saturation state exceeds a prescribed saturation limit; in effect, we constrain the ocean everywhere to be: $\Omega_{arg} \leq \Omega_{thresh}$. The results suggest that assuming an initial ocean saturation state of $\Omega_0 = 6.5$ (our baseline Neoproterozoic scenario), biologically-induced pelagic carbonate production may become significant for atmospheric CO_2 below ca. 2000 ppmv. It is possible that at the end of the Precambrian, the ocean saturation state was more similar to that of the modern ocean than we have previously argued. In this event, we find that with $\Omega_0 = 3.5$, pelagic carbonate production is unlikely to be important at any point, a consequence of the greater saturation gap between initial and threshold states. Our ability to determine whether CO_2 values could fall below ca. 500-2000 ppmv from an initial value of 3400 ppmv during Neoproterozoic glaciation lies within the uncertainties in knowing Precambrian ocean chemistry and the dynamics of biologically-induced $CaCO_3$ precipitation that pelagic carbonate precipitation.

5.3 The Importance of Feedbacks in the System

Thus far, our analysis has excluded the role of positive feedbacks in the Earth system, which will act to enhance the importance of the carbonate depositional mechanism. For instance, we have assumed that all carbonate, once deposited in the neritic environment is, in effect, isolated from the system. However, when sub-aerially exposed following a fall in sea level, previously deposited carbonates will be subject to erosion [*Munhoven and François*, 1996; *Walker and Opdyke*, 1995]. That this may have occurred associated with the development of glaciation in the Neoproterozoic is consistent with carbon isotopic evidence for platform carbonate truncation in the uppermost Ombaatjie Formation (Namibia) [*Halverson et al.*, 2002]. We test the potential importance of this effect by assuming that previously deposited carbonate units lying above sea level weather at a basic rate of 1.1 mol $CaCO_3$ m^{-2} a^{-1} [*Munhoven and François*, 1996]. This rate is then modified according to the GEOCARB (pre-vascular plant) weathering rate formulation [*Berner*, 1990] as per the riverine DIC and ALK fluxes to the ocean. The results of this are shown in Figure 6. Erosion of previously-deposited carbonates now drives a CO_2 drawdown to a minimum of 651 ppmv (compared to 1377 ppmv in the baseline case) as the excess CO_3^{2-} supply forces the ocean aqueous carbonate equilibrium, $CO_2 + CO_3^{2-} + H_2O \leftrightarrow 2HCO_3^-$ further to the right to compensate. Initial atmospheric CO_2 drawdown also takes place noticeably more rapidly.

It could be argued that the importance of this carbonate erosion term is already implicit in our earlier assumption that an increase in terrestrial ice cover has no significant impact on the global weathering rate. The basic reasoning behind this is that at the Last Glacial Maximum, the land area lost to increased ice sheet cover is approximately compensated for by the area of exposed continental shelves [*Gibbs and Kump*, 1994]. If area were the only important factor, adding an explicit erosion feedback term runs the risk of counting the weathering of former neritic carbonates twice. However, the shelves contain a disproportionate fraction of carbonate rock compared to global mean lithology. This tends to be relatively recently deposited material and so is also more susceptible to weathering compared to the global average. The potential importance of these factors is reflected in the 20-30% higher bicarbonate flux to the ocean predicted during glacial compared to interglacial periods in the Quaternary glacial geochemical system [*Gibbs and Kump*, 1994; *Jones et al.*, 2002; *Munhoven*, 2002]. We therefore regard the results of the 'with-erosion' (Figure 6) scenario as a maximum end-member effect. The impact of carbonate erosion is likely to be more important during the earlier stages of ice sheet growth, when the area lost due to ice sheet growth will tend to be much less than the epicratonic area exposed by the resulting fall in sea level.

A more fundamental enhancement of the impact of incipient glaciation on atmospheric CO_2 arises through positive feedback between the carbon cycle and climate system. Two feedback loops are identified; (i) reduced neritic deposition $\rightarrow$ increased $[CO_3^{2-}]$ $\rightarrow$ lower atmospheric CO_2 $\rightarrow$ cooling $\rightarrow$ ice sheet growth and further sea level fall $\rightarrow$ reduced neritic deposition, and (ii) lower atmospheric CO_2 $\rightarrow$ cooling $\rightarrow$ higher ocean surface CO_2 solubility $\rightarrow$ lower atmospheric CO_2. These are shown schematically in Figure 9.

Because the atmosphere-ocean-sediment carbon cycle model already implicitly calculates the response of atmospheric CO_2 to; (i) sea level, and (ii) sea surface temperatures (SST), the role of these feedbacks can be accounted for by incorporating just two additional parameterizations. These parameterizations represent the sensitivity to a reduction in atmospheric CO_2 of; (i) ice sheet volume (and thus sea level), and (ii) SST, and thus 'close' the feedback loops. To construct these parameterizations we utilize the climate system sensitivity to a reduction in radiative forcing exhibited by coupled ice-sheet climate models [*Berger and Loutre*, 1997; *Berger et al.*, 1998; *Crowley et al.*, 2000; *Hyde et al.*, 2000]. The first relationship is formulated as a regression of global ice volume (V) against radiative cooling ΔQ_{CO2} (Figure 10). We then relate ice volume to sea level change assuming 45×10^6 km^3 land-based ice corresponds to 120 m lower sea level. Radiative forcing is related to CO_2 using standard expressions [*Ramaswamy et al.*, 2001]. For the second feedback relationship, because the change in mean global surface temperature is not far from linear with radiative forcing (at least across the range of radiative forcings of interest here) [*Crowley et al.*, 2000; *Hyde et al.*, 2000], we make the approximation; $\Delta SST = 0.64 \times \Delta Q_{CO2}$.

The effect of accounting for these two fundamental climatic feedbacks, both individually and in combination is shown in Figure 11. Operation of the SST feedback in isolation has a relatively modest effect, driving an additional 169 ppmv CO_2 drawdown compared to the baseline scenario (Figure 6), giving a minimum of 1208 ppmv. In contrast, the ice volume feedback is much stronger and increases the CO_2 draw-down to a minimum of 1004 ppmv. The ice volume feedback concurrently drives a maximum sea level fall of 310 m, corresponding to an increase in global ice volume to 116×10^6 km^3 and almost three times the maximum late Quaternary glacial-interglacial difference of 40-50×10^6 km^3 [*Berger and Loutre*, 1997]. With both feedbacks operating in combination there is further CO_2 drawdown and sea level fall, with respective minima of 867 ppmv and -344 m. Importantly, under the influence of both feedbacks combined, an initial -50 m perturbation of sea level is sufficient to produce substantial drawdown in atmospheric CO_2, with a minimum of 846 ppmv achieved (not shown). Even if a modern topographic profile is assumed, an initial -50 m perturbation of sea level gives 1523 ppmv upon inclusion of these feedbacks (also not shown).

An important aspect of our analysis is the slow recovery time of the system from low CO_2. We find a time scale of $>10^6$ years for the negative feedback due to silicate weathering in the Precambrian. This compares to 0.2-0.3×10^6 years previously estimated for the late Phanerozoic [*Archer et al.*, 1997, 1998; *Caldeira and Rampino*, 1993]). This can be understood partly in terms of the more extreme ocean chemistry required consistent with both high atmospheric CO_2 [*Crowley et al.*, 2001; *Hyde et al.*, 2000; *Jenkins and Smith*, 1999] and a supersaturated Precambrian ocean [*Arp et al.*, 2001; *Grotzinger and Knoll*, 1995; *Riding*, 2000] (see Section 4; "A model for Neoproterozoic CO_2"). The extended residence time of mantle and metamorphically-generated carbon in a system with an initial carbon inventory more than four times present then produces a damped feedback response. The two negative (weathering and neritic precipitation) feedbacks also interact antagonistically. For instance, an incremental increase in atmospheric CO_2 driven by 'excess' CO_2 out-gassing will make the ocean more acidic and suppress the degree of supersaturation, Ω_{arg}. The resulting reduction in $CaCO_3$ removal in neritic environments will act to restore Ω_{arg} and thus reverse much of the original atmospheric CO_2 increase. As a result of these factors, a low CO_2 state persists for millions of years. That Precambrian ocean chemistry should deviate sufficiently from the modern system to weaken the silicate weathering feedback on climate and allow long-lived and stable glaciation has not previously been recognized.

6. MAGNITUDE AND STABILITY OF NEOPROTEROZOIC ICE AGES, AND OCCURRENCE OF 'CAP' CARBONATES

6.1 The Occurrence of Extreme Ice Ages

In the absence of planktic calcifiers, the high degree of sensitivity to sea level change of atmospheric CO_2 and radiative forcing has far-reaching implications for understanding Neoproterozoic glaciation. We hypothesize that cooling and incipient ice cap growth during the Neoproterozoic triggered our carbonate depositional mechanism. Loss of depositional environments (and associated feedbacks) was then directly responsible for the unusual severity and longevity of these ice ages.

The required trigger is incipient glaciation and initial sea level fall; as limited as one third the maximum magnitude attained during the late Quaternary. A period of enhanced organic carbon burial is one possible mechanism for driving climatic cooling and incipient glaciation. This is consistent with observations of highly enriched carbonate $\delta^{13}C$ immediately prior to glaciation [*Hoffman et al.*, 1998; *Hoffman and Schrag*, 2002; *Kennedy et al.*, 1998]. Suggestions for the driver for this organic carbon burial event include an enhanced weathering flux of phosphorous to the ocean associated with hypothesized early plant colonization of land [*Lenton and Watson*, submitted]. Catastrophic cooling due to the sudden loss of a 'methane greenhouse' [*Schrag et al.*, 2002], CO_2 drawdown from the weathering of extensive fresh basaltic provinces [*Goddéris et al.*, 2003], and reduced insolation in the aftermath of a comet/asteroid impact [*Bendtsen and Bjerrum*, 2002] are other alternatives that have been suggested.

We favor a fundamental role for supercontinent formation and fragmentation phases which, in driving substantial changes in continental emergence/submergence [*Crowell*, 1999] provide the necessary topographic boundary conditions. Relocation of substantial continental area to the pole, or to the tropics (where enhanced weathering could drive CO_2 draw-down and achieve the necessary cooling threshold [*Goddéris et al.*, 2003]) would be consistent with this view. Indeed, it has been noted that episodes of Neoproterozoic glaciation are separated on a tectonic timescale [*Hoffman and Schrag*, 2002; *Kennedy et al.*, 1998; *Prave*, 1999], compatible with an overall tectonic control on the timing of glaciation. The apparent ca. 1000 Ma absence of severe glaciation prior to the Neoproterozoic [*Brasier and Lindsey*, 1998; *Crowell*, 1999] may then be due to an absence of sufficient topographic contrast in the earlier Proterozoic. An absence of extensive rifting episodes, for instance, could explain this. Unsuitable hypsometry might also help explain why glaciation at the end Ordovician was comparatively 'mild' and short lived [*Brenchley et al.*, 1994; *Crowell*, 1999], although a change in carbonate deposition with the advent of carbonate secreting organisms (metazoans) at the Precambrian-Cambrian boundary is likely to be critical [*Ridgwell et al.*, 2003].

Glaciation has been a frequent feature throughout the Phanerozoic, and has a wide variety of suspected causes [*Crowell*, 1999]. That glaciation should also occur during the Neoproterozoic is not entirely surprising. What is unusual, however, is the severity and inferred duration of the recorded ice ages. It is this aspect of the geological record that is explicitly explained by our model, rather than the initial occurrence of glaciation and sea level fall *per se*.

Thus, given a suitable incipient glacial trigger, we predict a dramatic reduction in the concentration of CO_2 in the atmosphere to a persistently low value in the range 800-1400 ppmv (Figures 6,11). This is a robust result with respect to a range of different model assumptions, including; (a) the dependence of $CaCO_3$ precipitation rate on ambient $[CO_3^{2-}]$ (the parameter '*n*'), (b) erosion of previously deposited carbonates when sub-aerially exposed, and (c) the action of sea surface temperature and ice volume/sea level feedbacks. We find that model-predicted glacial CO_2 corresponds well with the "CO_2 attractor" of radiative forcing parameter space of *Baum and Crowley* [2001]; equivalent to ~×2.5 to ×4.5 'present-day' level (PAL) of CO_2 ,or 850 to 1530 ppmv assuming 1.0 PAL = 340 ppmv. This degree of radiative forcing gives rise to an open equatorial ocean coexisting with low latitude ice sheets in GCM and coupled climate-ice sheet models [*Baum and Crowley*, 2001]. With an open equatorial ocean there would be an active hydrological cycle, which is fully consistent with observed characteristics of glacial diamictite deposition [*Arnaud and Elyes*, 2002; *Condon et al.*, 2002; *Leather et al.*, 2002; *McMechan*, 2000]. Furthermore, multicellular life would have survived in the refugium provided by an equatorial belt of open water [*Hyde et al.*, 2000, 2001; *Runnegar*, 2000].

Our sensitivity analyses suggest that CO_2 concentrations low enough to cross the threshold required for sea-ice instability and run-away ice-albedo feedback into a 'snowball Earth' are difficult to achieve. In many climate models that exhibit a sea-ice instability, this threshold is found somewhere below ca. 340 ppmv (×1.0 PA) [*Crowley et al.*, 2001; *Goddéris et al.*, 2003; *Hyde et al.*, 2000]. Clearly, our analysis of the Precambrian carbon cycle is not exhaustive – there may be further mechanisms and feedbacks that would act to enhance the CO_2 draw-down resulting from an initial fall in sea level. However, analysis of the potential role of pelagic precipitation carried out earlier (Figure 8) suggests that there is a fundamental limitation on the degree of over-saturation (and thus CO_2 draw-down) that can be achieved in the ocean. Although the uncertainties are substantial, the associated minimum limit placed on atmospheric CO_2 may be ca. ≥500 ppmv (from an initial state of 3400 ppmv). On time scales of ca. < 1 Myr, the Neoproterozoic global carbon cycle may therefore be inherently unable to provide the radiative cooling necessary for rapid development of 'snowball' glaciation through atmospheric CO_2 draw-down. The occurrence of 'snowball Earth' conditions therefore requires that more exotic and speculative means of global cooling, such as the sudden loss of a methane 'greenhouse' [*Schrag et al.*, 2002] be invoked.

In our model, the glacial period would have persisted until reduced silicate weathering brought the system to a radiative (CO_2) threshold for deglaciation, analogous to the mechanism proposed for the termination of Late Ordovician glaciation [*Kump et al.*, 1999]. We predict that the period of time required for this would have been of the order of millions of years, consistent with the inferred duration of the glaciation [*Hoffman et al.*, 1998; *Hoffman and Schrag*, 2002]. However, in the absence of explicit representation of the interactive response of the climate-cryosphere-lithosphere system, the timing of deglaciation cannot be predicted *a priori* by our current model. We therefore artificially impose a reversal of the initial sea level change after 2 Myr to simulate deglaciation (Figure 12A). This leads us to a further important piece of the Neoproterozoic jigsaw.

6.2 The Origin of the 'Cap' Carbonates

An explicit prediction of our hypothesis is that a relationship should exist between the thickness of post-glacial 'cap' (dolostone) carbonate facies and the 'excess' alkalinity accumulated in the ocean during the glacial as a result of loss of shallow water depositional environments. We find that within 5×10^4 years of deglaciation, $2.8\text{-}7.1\times10^{18}$ mol eq of accumulated alkalinity ($1.4\text{-}3.5\times10^{18}$ mol $CaCO_3$) is lost through excess deposition in neritic environments, with over half occurring in less than 10^4 years (Figure 12B). Assuming a postglacial neritic area of 6.1×10^7 km^2 (three times the area of the present-day shelf), this is sufficient to form a carbonate layer averaging between 0.8 and 2.1 m thick, assuming a density for aragonite of 2.9 g cm^{-3}, and zero initial porosity. The range and maximum thickness of carbonate would be considerably extended with heterogeneous distribution of the deposition, both with latitude (precipitation in warm tropics favored over that in colder polar regions) and depth (warmer shallow sunlit platforms favored over cooler deeper basins). Any porosity associated with initial precipitation and only subsequently infilled by secondary cements would also increase the effective thickness of the facies predicted by our model.

Although we chose to apply the sea level rise over an interval of 1 kyr in this analysis, by analogy with the late Quaternary, ice sheet collapse would be rapid and could be largely complete within just ~5 kyr [*Fairbanks*, 1989]. Assuming this slightly longer period of sea level rise has little effect on the total mass of $CaCO_3$ deposited. However, a slower rate of sea level rise would help account for the observed variability in 'cap' thickness, as lower-lying areas would be flooded earlier and thus experience the higher initial degree of saturation (and more rapid precipitation).

Regardless of possible modifying factors, our quantitative predictions coincide with typical 'cap' (dolostone) carbonate facies thicknesses observed in shelfal settings of order meters [*Grotzinger and Knoll*, 1995; *James et al.*, 2001; *Kennedy*, 1996; *Kennedy et al.*, 1998; *Kennedy et al.*, 2001b; *Myrow and Kaufman*, 1999]. Thus, the timing, thickness, and inferred rapid precipitation of 'cap' carbonate is consistent with a 'coral reef' like mechanism [*Kennedy*, 1996], with rapid deposition on newly flooded continental shelves taking place from a highly oversaturated ocean.

Because the glacial ocean is characterized by a high degree of super-saturation, any hiatus in the deposition of glaciogenic sedimentary material could allow the formation of sufficient *in situ* carbonate precipitation to form identifiable features in the geological record. The restrictive area afforded by the continental slope for deposition at low glacial sea level stand will produce a strong sampling bias against finding such evidence. In spite of this, distinctive *in situ* synglacial carbonates have been observed [*Kennedy et al.*, 2001a]. Such evidence is incompatible with the undersaturated to (no greater than) marginally saturated glacial ocean that is possible during a 'snowball Earth' like event [*Higgins and Schrag*, 2003; *Hoffman and Schrag*, 2002].

7. A 'SLUSHBALL EARTH' WITH CAP CARBONATES?

Where does this analysis leave the viability of an open ocean 'slushball' interpretation of Neoproterozoic glaciation as an alternative to the extreme deep freeze of a 'snowball Earth'? Both the magnitude and longevity of the glacial, as well as the post-glacial deposition of the enigmatic 'cap' carbonates can be understood in terms of weak 'buffering' of the Precambrian carbon cycle [*Ridgwell et al.*, 2003b]. Because the radiative forcing necessary for low latitude ice sheets to co-exist with an open tropical ocean is consistent with the CO_2 draw-down predicted by our model, the requirements both for viable life to persist and active hydrological cycling to continue throughout the glacial period are also easily accommodated. All these key geological observations arise naturally from the dynamics of a Precambrian carbon cycle in the absence of pelagic calcifiers, and do not require invocation of a specific sequence of poorly supported geochemical and climatic conditions. Our model of carbonate depositional control therefore helps provide a more parsimonious explanation of Neoproterozoic glaciation than does a 'snowball Earth'.

Acknowledgments. Both authors would like to thank NSF EAR for financial support, Ken Caldeira for advice on modeling strategies, and helpful feedback provided by various colleagues, with particular thanks to; Nick Christie-Blick, Sören Jensen, Bob Gaines, and Seth Finnegan. As the University of East Anglia

'John Peyton Research Fellow', AJR would like to acknowledge the Trusthouse Charitable Foundation for providing additional financial assistance.

REFERENCES

Algeo, T. J., K. B. Seslavinsky, The paleozoic world - Continental flooding, hypsometry, and sealevel, *American Journal of Science*, 295, 787-822, 1995.

Archer, D., H. Kheshgi, and E. Maier-Reimer, Multiple timescales for neutralization of fossil fuel CO_2, *Geophysical Research Letters*, 24, 405-408, 1997.

Archer, D., H. Kheshgi, and E. Maier-Reimer, Dynamics of fossil fuel CO_2 neutralization by marine $CaCO_3$, *Global Biogeochemical Cycles*, 12, 259-276, 1998.

Arnaud, E., C. H. Eyles, Glacial influence on Neoproterozoic sedimentation: The Smalfjord Formation, northern Norway, *Sedimentology*, 49, 765-788, 2002.

Arp, G., V. Thiel, A. Reimer, W. Michaelis, J. Reitner, Biofilm exopolymers control microbialite formation at thermal springs discharging into the alkaline Pyramid Lake, Nevada, USA, *Sedimentary Geology*, 126, 159-176, 1999.

Arp, G., A. Reimer, J. Reitner, Photosynthesis-induced biofilm calcification and calcium concentrations in Phanerozoic oceans, *Science*, 292, 1701-1704, 2001.

Arp, G., A. Reimer, J. Reitner, Microbialite formation in seawater of increased alkalinity, Satonda crater lake, Indonesia, *J. Sed. Res*, 73, 105-127, 2003.

Barker, S., H. Elderfield, Foraminiferal calcification response to glacial-interglacial changes in atmospheric CO_2, *Science*, 297, 833-836, 2002.

Baum, S. K., T. J. Crowley, GCM response to late Precambrian (similar to 590 Ma) ice-covered continents, *Geophysical Research Letters*, 28, 583-586, 2001.

Bendtsen, J., Climate sensitivity to changes in solar insolation in a simple coupled climate model, *Climate Dynamics*, 18, 595-609, 2002.

Bendtsen, J., and C. J. Bjerrum, Vulnerability of climate on Earth to sudden changes in insolation, *Geophysical Research Letters*, 29, doi:10.1029/2002GL014829, 2002.

Berger, A., X. S. Li, and M. F. Loutre, Modelling northern hemisphere ice volume over the last 3 Ma, *Quaternary Science Reviews*, 18, 1-11, 1999.

Berger, A., M. F. Loutre, H. Gallee, Sensitivity of the LLN climate model to the astronomical and CO_2 forcings over the last 200 ky, *Climate Dynamics*, 14, 615-629, 1998.

Berger, W. H., Increase of carbon dioxide in the atmosphere during deglaciation: The coral reef hypothesis, *Naturwissenschaften*, 69, 87-88, 1982.

Berner, R. A., Atmospheric carbon-dioxide levels over Phanerozoic time, *Science*, 249, 1382-1386, 1990.

Boss, S. K., A. C. Neumann, Physical versus chemical processes of whiting formation in the Bahamas, *Carbonate and Evaporites*, 8, 135-148, 1993.

Boss, S. K., B. H. Wilkinson, Planktogenic eustatic control on cratonic oceanic carbonate accumulation, *Journal of Geology*, 99, 497-513, 1991.

Brasier, M. D., J. F. Lindsay, A billion years of environmental stability and the emergence of eukaryotes: New data from northern Australia, *Geology*, 26, 555-558, 1998.

Brenchley, P. J., Bathymetric and isotopic evidence for a short-lived late Ordovician glaciation in a greenhouse period, *Geology*, 22, 295-298, 1994.

Broecker, W. S., and T-H. Peng, Glacial to interglacial changes in the operation of the global carbon cycle, *Radiocarbon*, 28, 309-327, 1986.

Broecker, W. S., A. Sanyal, T. Takahashi, The origin of Bahamian whitings revisited, *Geophysical Research Letters*, 27, 3759-3760, 2000.

Budyko, M. I., The effect of solar radiation variations on the climate of the Earth, *Tellus*, 11, 611-619, 1969.

Burton, E. A., L. M. Walter, Relative precipitation rates of aragonite and mg calcite from seawater - Temperature or carbonate ion control, *Geology*, 15, 111-114, 1987.

Cahalan, R. F., G. R. North, A stability theorem for energy-balance climate models, *J. Atm. Sci.*, 36, 1178-1188, 1979.

Caldeira, A. K., J. F. Kasting, Susceptibility of the early Earth to irreversible glaciation caused by carbon dioxide clouds, *Nature*, 359, 226-228, 1992.

Caldeira, K., M. R. Rampino, Aftermath of the end-cretaceous mass extinction - possible biogeochemical stabilization of the carbon-cycle and climate, *Paleoceanography*, 8, 515-525, 1993.

Chandler, M. A., L. E. Sohl, Climate forcings and the initiation of low-latitude ice sheets during the Neoproterozoic Varanger glacial interval, *Journal of Geophysical Research – Atmospheres*, 105, 20737-20756, 2000.

Condon, D. J., A. R. Prave, D. I. Benn, Neoproterozoic glacial-rainout intervals: Observations and implications, *Geology*, 30, 35-38, 2002.

Crowell, J. C., Pre-Mesozoic Ice Ages: Their Bearing on Understanding the Climate System, *Mem. Geol. Soc. Am.*, 192, 1999.

Crowley, T. J., W. T. Hyde, W. R. Peltier, CO_2 levels required for deglaciation of a “Near-Snowball” Earth, *Geophysical Research Letters*, 28, 283-286, 2001.

Donnadieu, Y., F. Fluteau,, G. Ramstein, C. Ritz, J. Besse, Is there a conflict between the Neoproterozoic glacial deposits and the snowball Earth interpretation: an improved understanding with numerical modeling, *Earth and Planetary Science Letters*, 208, 101-112, 2003.

ETOPO5, Data Announcement 88-MGG-02, *Digital relief of the Surface of the Earth*. NOAA, National Geophysical Data Centre, Boulder, Colorado, 1988.

Evans, D. A. D., Stratigraphic, geochronological, and paleomagnetic constraints upon the Neoproterozoic climatic paradox, *American Journal of Science*, 300, 347-433, 2000.

Fairbanks, R. G., A 17,000-year glacio-eustatic sea level record: Influence of glacial melting rates on the Younger Dryas event and deep-ocean circulation, *Nature*, 342, 637-642, 1989.

Gibbs, M. T., L. R. Kump, Global chemical erosion during the last glacial maximum and present: Sensitivity to changes in lithology and hydrology, *Paleoceanography*, 9, 529-543, 1994.

Goddéris, Y., et al., The Sturtian ‘snowball’ glaciation: fire and ice, *Earth and Planetary Science Letters*, 211, doi:10.1016/S0012-821X(03)00197-3, 2003.

Grotzinger, J. P., N. P. James, Precambrian carbonates; Evolution of understanding, *In: Carbonate Sedimentology and Diagenesis in the Evolving Precambrian World*, SEPM, 2000.

Grotzinger, J. P., A. H. Knoll, Anomalous carbonate precipitates: Is the Precambrian the key to the Permian?, *Palaios*, 10, 578-596, 1995.

Halverson, G. P., P. F. Hoffman, D. P. Schrag, A. J. Kaufman, A major perturbation of the carbon cycle before the Ghaub glaciation (Neoproterozoic) in Namibia: a trigger mechanism for snowball Earth?, *Geochemistry, Geophysics Geosystems*, 2, DOI:10.1029/2001GC000244, 2002.

Heinrich, H., Origin and consequences of cyclic ice-rafting in the northeast Atlantic Ocean during the past 130 000 years, *Quaternary Research*, 29, 143–152, 1988.

Higgins, J. A., D. P. Schrag, Aftermath of a snowball Earth, *Geochemistry, Geophysics, Geosystems*, 4, DOI: 10.1029/2002GC000403, 2003.

Hoffman, P. F., Vreeland diamictites - Neoproterozoic glaciogenic slope deposits, Rocky Mountains, northeast British Columbia, *Bulletin of Canadian Petroleum Geology*, 48, 360-363, 2000.

Hoffman, P. F., A. J. Kaufman, G. P. Halverson, D. P. Schrag, A Neoproterozoic snowball earth, *Science*, 281, 1342-1346, 1998.

Hoffman, P. F., D. P. Schrag, The snowball Earth hypothesis: testing the limits of global change, *Terra Nova*, 14, 129-155, 2002.

Hyde, W. T., T. J. Crowley, S. K. Baum, W. R. Peltier, Neoproterozoic ‘snowball Earth’ simulations with a coupled climate/ice-sheet model, *Nature*, 405, 425-429, 2000.

Hyde, W. T., T. J. Crowley, S. K. Baum, W. R. Peltier, Life, geology and snowball Earth – reply, *Nature*, 409, 306, 2001.
Jacobsen, S. B., A. J. Kaufman, The Sr, C and O isotopic evolution of Neoproterozoic seawater, *Chemical Geology*, 161, 37-57, 1999.
James, N. P., G. M. Narbonne, T. K. Kyser, Late Neoproterozoic cap carbonates: Mackenzie Mountains, northwestern Canada: precipitation and global glacial meltdown, *Canadian Journal of Earth Sciences*, 38, 1229-1262, 2001.
Jenkins, G. S., S. R. Smith, GCM simulations of Snowball Earth conditions during the late Proterozoic, *Geophysical Research Letters*, 26, 2263-2266, 1999.
Jones, I. W., G. Munhoven, M. Tranter, P. Huybrechts, M. J. Sharp, Modelled glacial and non-glacial HCO_3^-, Si and Ge fluxes since the LGM: little potential for impact on atmospheric CO_2 concentrations and a potential proxy of continental chemical erosion, the marine Ge/Si ratio, *Global and Planetary Change*, 33, 139-153, 2002.
Kennedy, M. J., Stratigraphy, sedimentology, and isotopic geochemistry of Australian Neoproterozoic postglacial cap dolostones: Deglaciation, delta C-13 excursions, and carbonate precipitation, *Journal of Sedimentary Research*, 66, 1050-1064, 1996.
Kennedy, M. J., B. Runnegar, A. R. Prave, K. H. Hoffmann, M. A. Arthur, Two or four Neoproterozoic glaciations?, *Geology*, 26, 1059-1063, 1998.
Kennedy, M. J., N. Christie-Blick, A. R. Prave, Carbon isotopic composition of Neoproterozoic glacial carbonates as a test of paleoceanographic models for snowball Earth phenomena, *Geology*, 29, 1135-1138, 2001a.
Kennedy, M. J., N. Christie-Blick, L. E. Sohl, Are Proterozoic cap carbonates and isotopic excursions a record of gas hydrate destabilization following Earth's coldest intervals?, *Geology*, 29, 443-446, 2001b.
Kirschivink, J. L., Late Proterozoic low-latitude global glaciation: the snowball Earth, *In: The Proterozoic Biosphere* (Schopf, J. W., Klein, C., eds), pp. 51-52, Cambridge University Press, Cambridge , 1992.
Kump, L. R., *et al.*, A weathering hypothesis for glaciation at high atmospheric pCO_2 during the Late Ordovician, *Palaeogeography, Palaeoclimatology, Palaeoecology*, 152, 173-187, 1999.
Leather, J., P. A. Allen, M. D. Brasier, A. Cozzi, Neoproterozoic snowball earth under scrutiny: Evidence from the Fiq glaciation of Oman, *Geology*, 30, 891-894, 2002.
Leclercq, N., J. P. Gattuso, J. Jaubert, CO_2 partial pressure controls the calcification rate of a coral community, *Global Change Biology*, 6, 329-334, 2000.
Lebrón, I., D. L. Suárez, Calcite nucleation and precipitation kinetics as affected by dissolved organic matter at 25 degrees C and pH>7.5, *Geochimica et Cosmochimica Acta*, 60, 2765-2776, 1996.
Lebrón, I., D. L. Suárez, Kinetics and mechanisms of precipitation of calcite as affected by P-CO2 and organic ligands at 25 degrees C, *Geochimica et Cosmochimica Acta*, 62, 405-416, 1998.
Lenton, T. M., A. J. Watson, Biotic enhancement of weathering, atmospheric oxygen and carbon dioxide in the Neoproterozoic, *submitted*.
Marshall, A. T., P. L. Clode, Effect of increased calcium concentration in sea water on calcification and photosynthesis in the scleractinian coral *Galaxea fascicularis*, *Journal of Experimental Biology*, 205, 2107-2113, 2002.
McMechan, M. E., Vreeland diamictites - Neoproterozoic glaciogenic slope deposits, Rocky Mountains, northeast British Columbia, *Bulletin of Canadian Petroleum Geology*, 48, 246-261, 2000.
Milliman, J. D., Production and accumulation of calcium carbonate in the ocean: Budget of a nonsteady state, *Global Biogeochemical Cycles*, 7, 927-957, 1993.
Milliman, J. D., A. W. Droxler, Neritic and pelagic carbonate sedimentation in the marine environment: Ignorance is not bliss, *Geologische Rundschau*, 85, 496-504, 1996.

Morse, J. W., D. K. Gledhill, F. J. Millero, $CaCO_3$ precipitation kinetics in waters from the Great Bahama Bank: Implications for the relationship between Bank, *Geochimica et Cosmochimica Acta*, 67, 2819-2826, 2003.

Morse, J. W., S. L. He, Influences of T, S and pCO_2 on the pseudo-homogeneous precipitation of $CaCO_3$ from seawater – Implications for whiting formation, *Marine Chemistry*, 41, 291-297, 1993.

Munhoven, G., Glacial-interglacial changes of continental weathering: estimates of the related CO_2 and HCO_3^- flux variations and their uncertainties, *Global and Planetary Change*, 33, 155-176, 2002.

Munhoven, G., and L. M. François, Glacial-interglacial variability of atmospheric CO_2 due to changing continental silicate rock weathering: A model study, *Journal of Geophysical Research*, 101, 21423-21437, 1996.

Myrow, P. M., A. J. Kaufman, A newly discovered cap carbonate above Varanger-age glacial deposits in Newfoundland, Canada, *Journal of Sedimentary Research*, 69, 784-793, 1999.

Opdyke, B. N., J. C. G. Walker, Return of the coral reef hypothesis: Basin to shelf partitioning of $CaCO_3$ and its effect on atmospheric CO_2, *Geology*, 20, 730-736, 1992.

Opdyke, B. N., B. H Wilkinson, Carbonate mineral saturation state and cratonic limestone accumulation, *American Journal of Science*, 293, 217-234, 1993.

Poulsen, C. J., Absence of a runaway ice-albedo feedback in the Neoproterozoic, *Geology*, 31, 473–476, 2003.

Poulsen, C. J., R. T. Pierrehumbert, R. L. Jacob, Impact of ocean dynamics on the simulation of the Neoproterozoic "snowball Earth", *Geophysical Research Letters*, 28, DOI: 10.1029/2000GL012058, 2001.

Poulsen, C. J., R. L. Jacob, R. T. Pierrehumbert, T. T. Huynh, Testing paleogeographic controls on a Neoproterozoic snowball Earth, *Geophysical Research Letters*, 29, DOI: 10.1029/2001GL014352, 2002.

Prave, A. R., Two diamictites, two cap carbonates, two delta C-13 excursions, two rifts: The Neoproterozoic Kingston Peak Formation, Death Valley, California, *Geology*, 27, 339-342, 1999.

Prave, A. R., Life on land in the Proterozoic: Evidence from the Torridonian rocks of northwest Scotland, *Geology*, 30, 811-814, 2002.

Ramaswamy, V., O. Boucher, J. Haigh, D. Hauglustaine, J. Haywood, G. Myhre, T. Nakajima, G.Y. Shi and S. Solomon, Radiative forcing of climate change, *in Climate Change 2001: The Scientific Basis: Contribution of WGI to the Third Assessment Report of the IPCC*, edited by J.T. Houghton et al., pp. 349-416, Cambridge University Press, New York, 2001.

Ridgwell, A. J., Glacial-interglacial perturbations in the global carbon cycle, PhD thesis, Univ. of East Anglia at Norwich, UK, 2001. (http://tracer.env.uea.ac.uk/e114/ridgwell_2001.pdf)

Ridgwell, A. J., A. J. Watson, and D. E. Archer, Modelling the response of the oceanic Si inventory to perturbation, and consequences for atmospheric CO_2, *Global Biogeochemical Cycles*, 16, 1071, DOI:10.1029/2002GB001877, 2002.

Ridgwell, A. J., A. J. Watson, M. A. Maslin, J. O. Kaplan, Implications of coral reef buildup for the controls on atmospheric CO_2 since the Last Glacial Maximum, *Paleoceanography*, 18, doi:10.1029/2003PA000893, 2003a.

Ridgwell, A. J., M. J. Kennedy, K. Caldeira, Carbonate deposition, climate stability, and Neoproterozoic ice ages, *Science*, 302, 859-682, 2003b.

Riding, R., Microbial carbonates: the geological record of calcified bacterial-algal mats and biofilms, *Sedimentology*, 47, 179-214, 2000.

Riebesell, U., I. Zondervan, B. Rost, P. D. Tortell, R. E. Zeebe, F. M. M. Morel, Reduced calcification of marine plankton in response to increased atmospheric CO_2, *Nature*, 407, 364-367, 2000.

Robbins, L. L., P. L. Blackwelder, Biochemical and ultrastructural evidence for the origin of whitings – A biologically induced cal-

cium-carbonate precipitation mechanism, *Geology*, 20, 464-468, 1992.
Robbins, L. L., Y. Tao, C. A. Evans, Temporal and spatial distribution of whitings on Great Bahama Bank and a new lime mud budget, *Geology*, 25, 947-950, 1997.
Runnegar, B., Loophole for snowball earth, *Nature*, 405, 403-404, 2000.
Schiebel, R., Planktic foraminiferal sedimentation and the marine calcite budget, *Global Biogeochemical Cycles*, 16, DOI: 10.1029/2001GB001459, 2002.
Schrag, D. P., P. F. Hoffman, Life, geology and snowball Earth, *Nature*, 409, 306, 2001.
Schrag, D. P., R. A. Berner, P. F. Hoffman, G. P. Halverson, On the initiation of a snowball Earth, *Geochemistry, Geophysics, Geosystems*, 3, DOI: 10.1029/2001GC000219, 2002.
Sohl, L. E., N. Christie-Blick, D. V. Kent, Paleomagnetic polarity reversals in Marinoan (ca. 600 Ma) glacial deposits of Australia: Implications for the duration of low-latitude glaciation in neoproterozoic time, *Geological Society of America Bulletin*, 111, 1120-1139, 1999.
Walker, J. C. G., and B. C. Opdyke, Influence of variable rates of netiric carbonate deposition on atmospheric carbon dioxide and pelagic sediments, *Paleoceanography*, 10, 415-427, 1995.
Willimas, G. E., Sediemntology, stable isotope geochemistry and paleoenvironment of dolostones capping late Precambrian glacial sequences in Australia, *Geological Society of Australia*, 26, 377-386, 1979.
Wood, R. A., J. P. Grotzinger, J. A. D. Dickson, Proterozoic modular biomineralized metazoan from the Nama Group, Namibia, *Science*, 296, 2383-2386, 2002.
Zeebe, R. E., and D. Wolf-Gladrow, *CO_2 in seawater: Equilibrium, kinetics, isotopes*, Elsevier Oceanographic Series 65, Elsevier, New York, 2001.
Zhong, S. J., A. Mucci, Calcite precipitation in seawater using a constant addition technique - a new overall reaction kinetic expression, *Geochimica et Cosmochimica Acta*, 57, 1409-1417, 1993.
Zuddas, P., A. Mucci, Kinetics of calcite precipitation from seawater .1. A classical chemical-kinetics description for strong electrolyte-solutions, *Geochimica et Cosmochimica Acta*, 58, 4353-4362, 1994.
Zuddas, P., A. Mucci, Kinetics of calcite precipitation from seawater: II. The influence of the ionic strength, *Geochimica et Cosmochimica Acta*, 62, 757-766, 1998.

M. J. Kennedy, Department of Earth Sciences, University of California - Riverside, Riverside, CA 92521, USA (martink@mail.ucr.edu).

A. J. Ridgwell, Department of Earth Sciences, University of California - Riverside, Riverside, CA 92521, USA (andyr@citrus.ucr.edu).

FIGURE CAPTIONS

Figure 1. Distribution of surface area of the Earth with altitude. The modern mean global hypsographic curve [*ETOTO5*, 1988] is shown plotted in black. This is characterized by gently sloping continental shelves which give way to comparatively steeper slopes at greater depth. The assumed depth interval (0 to -100 m) of the neritic (photic) zone of biologically induced carbonate deposition is shaded. Also shown is a hypothetical distribution (grey line) perhaps more representative of times during Neoproterozoic, with initial neritic area ×3 greater than in the modern distribution.

Figure 1. Distribution of surface area of the Earth with altitude. The modern mean global hypsographic curve [*ETOTO5*, 1988] is shown plotted in black. This is characterized by gently sloping continental shelves which give way to comparatively steeper slopes at greater depth. The assumed depth interval (0 to -100 m) of the neritic (photic) zone of biologically induced carbonate deposition is shaded. Also shown is a hypothetical distribution (grey line) perhaps more representative of times during Neoproterozoic, with initial neritic area ×3 greater than in the modern distribution.

Figure 2. Schematic of the Quaternary carbonate depositional system and operation of the 'coral reef' mechanism [*Berger*, 1982; *Munhoven and François*, 1996; *Ridgwell et al.*, 2003a; *Walker and Opdyke*, 1995].
(a) High sea level stand; steady state, with weathering input of Ca^{2+} and CO_3^{2-} balanced by burial of $CaCO_3$, partitioned between neritic and deep ocean environments. A substantial fraction of planktic $CaCO_3$ reaching surface sediments dissolves and is recycled back to the ocean.
(b) Low sea level stand with reduced neritic area. Imbalance between sources and sinks of CO_3^{2-} results in increasing ocean saturation (and decreasing atmospheric CO_2). Preservation and burial of $CaCO_3$ in deep-sea sediments is enhanced until the loss of neritic sink is compensated for, and the system attains a new steady state.

Figure 2. Schematic of the Quaternary carbonate depositional system and operation of the 'coral reef' mechanism [*Berger*, 1982; *Munhoven and François*, 1996; *Ridgwell et al.*, 2003a; *Walker and Opdyke*, 1995].
(a) High sea level stand; steady state, with weathering input of Ca^{2+} and CO_3^{2-} balanced by burial of $CaCO_3$, partitioned between neritic and deep ocean environments. A substantial fraction of planktic $CaCO_3$ reaching surface sediments dissolves and is recycled back to the ocean.
(b) Low sea level stand with reduced neritic area. Imbalance between sources and sinks of CO_3^{2-} results in increasing ocean saturation (and decreasing atmospheric CO_2). Preservation and burial of $CaCO_3$ in deep-sea sediments is enhanced until the loss of neritic sink is compensated for, and the system attains a new steady state.

Figure 3. Schematic of an idealized Precambrian carbonate depositional system.
(a) High sea level stand and relatively large neritic area of rift and intra-cratonic basins; steady state, with weathering input of Ca^{2+} and CO_3^{2-} balanced by burial of $CaCO_3$ solely in neritic environments.
(b) Low sea level stand with reduced neritic area. There is no deep-sea sedimentary carbon system to buffer the reduction in neritic deposition in this case.

Figure 3. Schematic of an idealized Precambrian carbonate depositional system.
(a) High sea level stand and relatively large neritic area of rift and intra-cratonic basins; steady state, with weathering input of Ca^{2+} and CO_3^{2-} balanced by burial of $CaCO_3$ solely in neritic environments.
(b) Low sea level stand with reduced neritic area. There is no deep-sea sedimentary carbon system to buffer the reduction in neritic deposition in this case.

Figure 4. Schematic of the chain of events initiated by a perturbation of sea level. Connections between the different system elements are shown as arrows. Connections can be characterized either by a positive correlation (i.e., an increase in the state of one component causes an increase in a second, or, a decrease in the state of one component causes a decrease in a second) shown in gray, or with a negative correlation (i.e., an increase in the state of one component causes a decrease in a second, or vice versa) shown in black. If a path of successive connections can be traced from any given component back to itself, a closed or 'feedback' loop is formed. An even number (including zero) of negatively correlated connections counted around the loop gives a positive feedback, which will act to amplify an initial perturbation in the state of any component within this loop. Conversely, an odd number of negative correlations give a negative feedback, which will tend to dampen any perturbation, thus stabilizing the system. Two negative feedback loops (consisting of one positive together with one negative correlation) between neritic $CaCO_3$ accumulation and ocean saturation state, $[CO_3^{2-}]$ (or to be more precise, the rate of increase of ocean $[CO_3^{2-}]$) and between atmospheric CO_2 and $[CO_3^{2-}]$ (the weathering feedback of *Berner* [1990]) act to stabilize the system against perturbation. Stabilization of oceanic $[CO_3^{2-}]$ though a third negative feedback involving deep sea $CaCO_3$ preservation (shown dotted) exists only in the Phanerozoic system.

Figure 4. Schematic of the chain of events initiated by a perturbation of sea level. Connections between the different system elements are shown as arrows. Connections can be characterized either by a positive correlation (i.e., an increase in the state of one component causes an increase in a second, or, a decrease in the state of one component causes a decrease in a second) shown in gray, or with a negative correlation (i.e., an increase in the state of one component causes a decrease in a second, or vice versa) shown in black. If a path of successive connections can be traced from any given component back to itself, a closed or 'feedback' loop is formed. An even number (including zero) of negatively correlated connections counted around the loop gives a positive feedback, which will act to amplify an initial perturbation in the state of any component within this loop. Conversely, an odd number of negative correlations give a negative feedback, which will tend to dampen any perturbation, thus stabilizing the system. Two negative feedback loops (consisting of one positive together with one negative correlation) between neritic $CaCO_3$ accumulation and ocean saturation state, $[CO_3^{2-}]$ (or to be more precise, the rate of increase of ocean $[CO_3^{2-}]$) and between atmospheric CO_2 and $[CO_3^{2-}]$ (the weathering feedback of *Berner* [1990]) act to stabilize the system against perturbation. Stabilization of oceanic $[CO_3^{2-}]$ though a third negative feedback involving deep sea $CaCO_3$ preservation (shown dotted) exists only in the Phanerozoic system.

Figure 5. Sensitivity of the carbon cycle to prescribed (-100 m) sea level forcing assuming modern hypsometry and a factor 3.2 reduction in neritic area.
(A) Predicted evolution of mean surface ocean saturation state (Ω_{arg}); with (dotted line) and without (dashed line) a responsive deep sea sedimentary carbonate sink, representing late Phanerozoic and Precambrian systems, respectively.
(B) Predicted evolution of atmospheric CO_2.

Figure 5. Sensitivity of the carbon cycle to prescribed (-100 m) sea level forcing assuming modern hypsometry and a factor 3.2 reduction in neritic area.
(A) Predicted evolution of mean surface ocean saturation state (Ω_{arg}); with (dotted line) and without (dashed line) a responsive deep sea sedimentary carbonate sink, representing late Phanerozoic and Precambrian systems, respectively.
(B) Predicted evolution of atmospheric CO_2.

Figure 6. Sensitivity of the carbon cycle to sea level change assuming modified hypsometry. Prescribed (-100 m) sea level forc-

ing as before, but now giving rise to a 10-fold reduction in neritic area upon sea level fall. Predicted evolution of atmospheric CO_2 is shown for different model assumptions regarding how strongly $CaCO_3$ precipitation rate responds to a change in ambient $[CO_3^{2-}]$; dotted, continuous, and (short) dashed lines corresponding to values of $n = 1.0$, $n = 1.7$ (baseline scenario), and $n = 2.5$, respectively. Also shown is the effect of erosion of previously-deposited carbonates with $n = 1.7$ (long dashed line). Atmospheric CO_2 concentrations relative to present atmospheric level (PAL) (and assuming 1.0 PAL = 340 ppmv) are highlighted, to indicate; initial conditions (×10 PAL), the "CO_2 attractor" of radiative forcing giving rise to ice-free equatorial waters coexisting with low latitude ice sheets (×2.5 PAL to ×4.5 PAL) [*Baum and Crowley*, 2001], and the approximate limit below which sea-ice instability and run-away ice-albedo feedback into a 'snowball Earth' has been predicted to occur (×1.0 PAL) [*Crowley et al.*, 2001; *Goddéris et al.*, 2003; *Hyde et al.*, 2000].

Figure 6. Sensitivity of the carbon cycle to sea level change assuming modified hypsometry. Prescribed (-100 m) sea level forcing as before, but now giving rise to a 10-fold reduction in neritic area upon sea level fall. Predicted evolution of atmospheric CO_2 is shown for different model assumptions regarding how strongly $CaCO_3$ precipitation rate responds to a change in ambient $[CO_3^{2-}]$; dotted, continuous, and (short) dashed lines corresponding to values of $n = 1.0$, $n = 1.7$ (baseline scenario), and $n = 2.5$, respectively. Also shown is the effect of erosion of previously-deposited carbonates with $n = 1.7$ (long dashed line). Atmospheric CO_2 concentrations relative to present atmospheric level (PAL) (and assuming 1.0 PAL = 340 ppmv) are highlighted, to indicate; initial conditions (×10 PAL), the "CO_2 attractor" of radiative forcing giving rise to ice-free equatorial waters coexisting with low latitude ice sheets (×2.5 PAL to ×4.5 PAL) [*Baum and Crowley*, 2001], and the approximate limit below which sea-ice instability and run-away ice-albedo feedback into a 'snowball Earth' has been predicted to occur (×1.0 PAL) [*Crowley et al.*, 2001; *Goddéris et al.*, 2003; *Hyde et al.*, 2000.

Figure 7. Sensitivity of the predicted atmospheric CO_2 minimum to the assumed initial CO_2 value. The 1:1 line is shown for comparison. Relative CO_2 draw-down (i.e., as a proportion of initial CO_2) is approximately independent of initial CO_2.

Figure 7. Sensitivity of the predicted atmospheric CO_2 minimum to the assumed initial CO_2 value. The 1:1 line is shown for comparison. Relative CO_2 draw-down (i.e., as a proportion of initial CO_2) is approximately independent of initial CO_2.

Figure 8. Effect of assumptions regarding the saturation threshold for pelagic carbonate precipitation on the predicted atmospheric CO_2 minimum. Shown is the system response with initial $\Omega_0 = 6.5$ (baseline scenario) and $\Omega_0 = 3.5$ (a saturation state much closer to that of the modern ocean).

Figure 8. Effect of assumptions regarding the saturation threshold for pelagic carbonate precipitation on the predicted atmospheric CO_2 minimum. Shown is the system response with initial $\Omega_0 = 6.5$ (baseline scenario) and $\Omega_0 = 3.5$ (a saturation state much closer to that of the modern ocean).

Figure 9. Schematic diagram of the $CaCO_3$-CO_2-sealevel feedback system for shallow water (neritic) carbonate depositional control of climate. Going clockwise around the loop, the primary feedback (sea level→neritic area→neritic $CaCO_3$ accumulation→$[CO_3^{2-}]$→atmospheric CO_2→temperature→ice volume→sea level) involves four negative correlations and three positive ones, so is positive overall, and will act to amplify an initial perturbation. The subsidiary feedback between CO_2 and (sea surface) temperature is also positive. The subsidiary negative feedbacks from Figure 4 have been omitted for clarity.

Figure 9. Schematic diagram of the $CaCO_3$-CO_2-sealevel feedback system for shallow water (neritic) carbonate depositional control of climate. Going clockwise around the loop, the primary feedback (sea level→neritic area→neritic $CaCO_3$ accumulation→$[CO_3^{2-}]$→atmospheric CO_2→temperature→ice volume→sea level) involves four negative correlations and three positive ones, so is positive overall, and will act to amplify an initial perturbation. The subsidiary feedback between CO_2 and (sea surface) temperature is also positive. The subsidiary negative feedbacks from Figure 4 have been omitted for clarity.

Figure 10. Ice sheet response to a radiative cooling of climate. Global ice volume predicted by coupled ice-sheet climate models [*Berger and Loutre*, 1997; *Berger et al.*, 1998; *Crowley et al.*, 2000; *Hyde et al.*, 2000] as a function of a change in radiative focing (ΔQ_{CO2}) with respect to an interglacial state. Data has been placed on a common scale of ΔQ_{CO2} where originally as a function of CO_2, assuming that $\Delta Q_{CO2} = 0$ corresponds to CO_2 of 3400 ppmv under reduced solar luminosity applicable to the Neoproterozoic [*Crowley et al.*, 2000; *Hyde et al.*, 2000], or relative to 340 ppmv under late Quaternary boundary conditions [*Berger and Loutre*, 1997; *Berger et al.*, 1998].

Figure 10. Ice sheet response to a radiative cooling of climate. Global ice volume predicted by coupled ice-sheet climate models [*Berger and Loutre*, 1997; *Berger et al.*, 1998; *Crowley et al.*, 2000; *Hyde et al.*, 2000] as a function of a change in radiative focing (ΔQ_{CO2}) with respect to an interglacial state. Data has been placed on a common scale of ΔQ_{CO2} where originally as a function of CO_2, assuming that $\Delta Q_{CO2} = 0$ corresponds to CO_2 of 3400 ppmv under reduced solar luminosity applicable to the Neoproterozoic [*Crowley et al.*, 2000; *Hyde et al.*, 2000], or relative to 340 ppmv under late Quaternary boundary conditions [*Berger and Loutre*, 1997; *Berger et al.*, 1998].

Figure 11. Effect of feedbacks in modifying the sensitivity of CO_2 to sea level change. The baseline model configuration is utilized in each case, i.e. initial 100 m sea level fall, modified bathymetry (10-fold reduction in neritic area), $n = 1.7$, no planktic calcifiers, and no explicit erosion.
(A) Prescribed basic -100 m sea level forcing (black line). Also shown is the resulting evolution of sea level under the influence of either sea level→neritic area→neritic $CaCO_3$ accumulation→$[CO_3^{2-}]$→atmospheric CO_2→temperature→ice volume→sea level feedback (dotted line), atmospheric CO_2→temperature→atmospheric CO_2 feedback (dashed line, but identical to the solid line of the baseline model and thus hidden), or both feedbacks combined (dot-dash line).
(B) Predicted evolution of atmospheric CO_2 under the influence of the same three feedback combinations, plus the baseline response (black line) for comparison. Atmospheric CO_2 concentrations are highlighted, to indicate; initial conditions (×10 PAL), the "CO_2 attractor" of radiative forcing giving rise to ice-free equatorial waters coexisting with low latitude ice sheets (×2.5 PAL to ×4.5 PAL) [*Baum and Crowley*, 2001], and the approximate limit below which sea-ice instability and run-away ice-albedo feedback into a 'snowball Earth' has been predicted to occur (×1.0 PAL) [*Crowley et al.*, 2001; *Goddéris et al.*, 2003; *Hyde et al.*, 2000].

Figure 11. Effect of feedbacks in modifying the sensitivity of CO_2 to sea level change. The baseline model configuration is utilized in each case, i.e. initial 100 m sea level fall, modified bathymetry (10-fold reduction in neritic area), $n = 1.7$, no planktic calcifiers, and no explicit erosion.
(A) Prescribed basic -100 m sea level forcing (black line). Also shown is the resulting evolution of sea level under the influence of either sea level→neritic area→neritic $CaCO_3$ accumulation→$[CO_3^{2-}]$→atmospheric CO_2→temperature→ice volume→sea level feedback (dotted line), atmospheric CO_2→temperature→atmospheric CO_2 feedback (dashed line, but identical to the solid line of the baseline model and thus hidden), or both feedbacks combined (dot-dash line).

(B) Predicted evolution of atmospheric CO_2 under the influence of the same three feedback combinations, plus the baseline response (black line) for comparison. Atmospheric CO_2 concentrations are highlighted, to indicate; initial conditions (×10 PAL), the "CO_2 attractor" of radiative forcing giving rise to ice-free equatorial waters coexisting with low latitude ice sheets (×2.5 PAL to ×4.5 PAL) [*Baum and Crowley*, 2001], and the approximate limit below which sea-ice instability and run-away ice-albedo feedback into a 'snowball Earth' has been predicted to occur (×1.0 PAL) [*Crowley et al.*, 2001; *Goddéris et al.*, 2003; *Hyde et al.*, 2000].

Figure 12. Response of alkalinity inventory to deglaciation.
(A) Sea level change, with a 100 m sea level rise applied after 2 Myr. Curves of the evolution of sea level are shown for the following model integrations (all assuming modified hypsometry); (i) baseline (n = 1.7), no erosion or feedbacks (solid line), (ii) n = 1.7, erosion but no feedbacks (long dashed line, but identical to the solid line of the baseline model and thus hidden), and (iii) n = 1.7, no erosion but both sea level→neritic area→neritic $CaCO_3$ accumulation→$[CO_3^{2-}]$→atmospheric CO_2→temperature→ice volume→sea level and atmospheric CO_2→temperature→atmospheric CO_2 feedbacks (dot-dashed line).
(B) Oceanic alkalinity (ALK) inventory. Rapid deglacial removal of alkalinity through carbonate precipitation is highlighted by an arrow.

Figure 12. Response of alkalinity inventory to deglaciation.
(A) Sea level change, with a 100 m sea level rise applied after 2 Myr. Curves of the evolution of sea level are shown for the following model integrations (all assuming modified hypsometry); (i) baseline (n = 1.7), no erosion or feedbacks (solid line), (ii) n = 1.7, erosion but no feedbacks (long dashed line, but identical to the solid line of the baseline model and thus hidden), and (iii) n = 1.7, no erosion but both sea level→neritic area→neritic $CaCO_3$ accumulation→$[CO_3^{2-}]$→atmospheric CO_2→temperature→ice volume→sea level and atmospheric CO_2→temperature→atmospheric CO_2 feedbacks (dot-dashed line).
(B) Oceanic alkalinity (ALK) inventory. Rapid deglacial removal of alkalinity through carbonate precipitation is highlighted by an arrow.

A CARBONATE DEPOSITIONAL CONTROL OF NEOPROTEROZOIC ICE AGES

ANDY RIDGWELL AND MARTIN KENNEDY

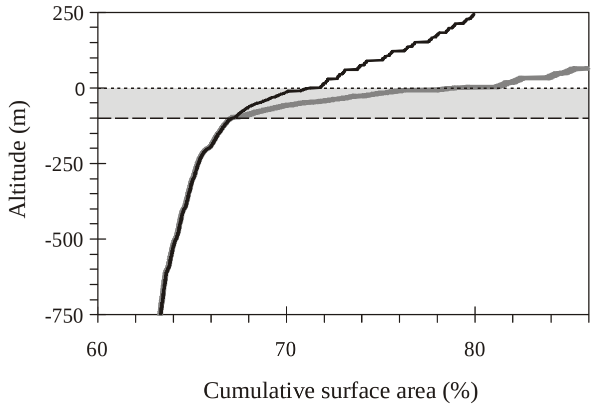

Ridgwell_Figure_01

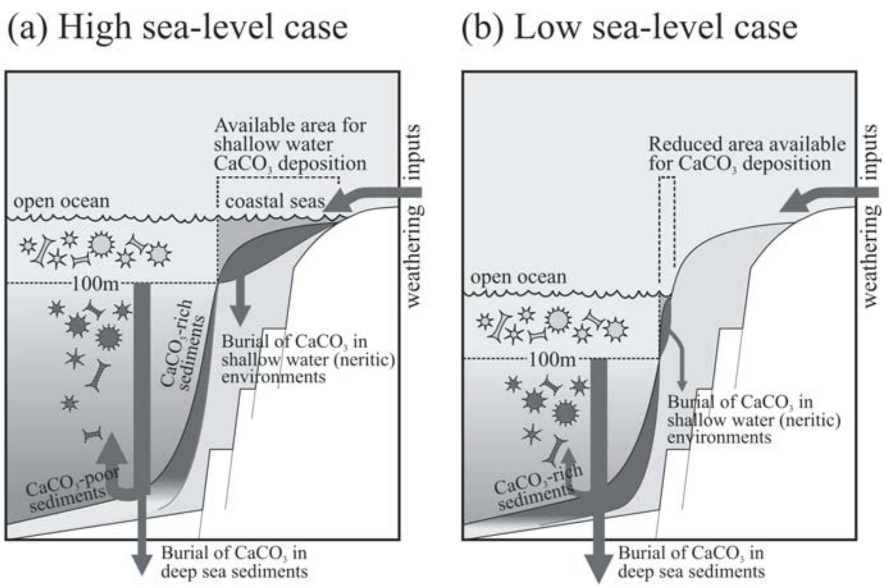

Ridgwell_Figure_02

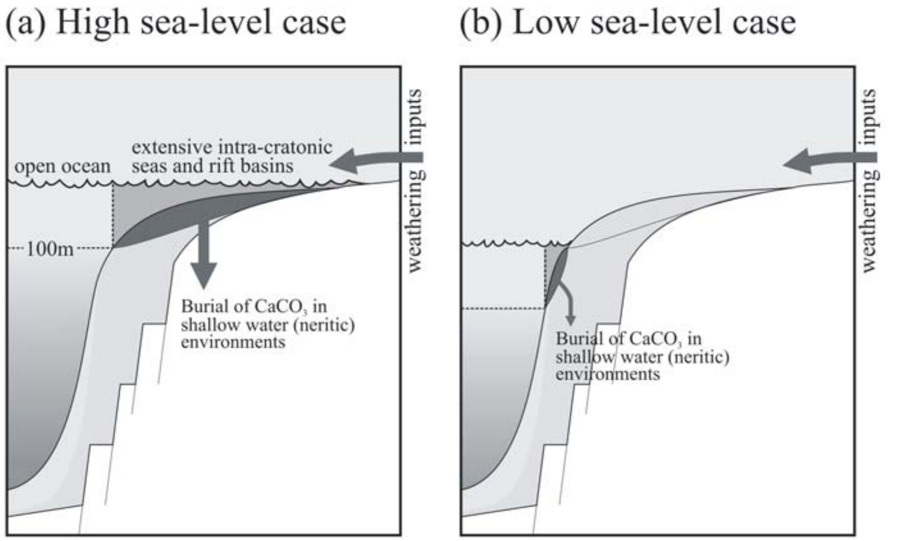

Ridgwell_Figure_03

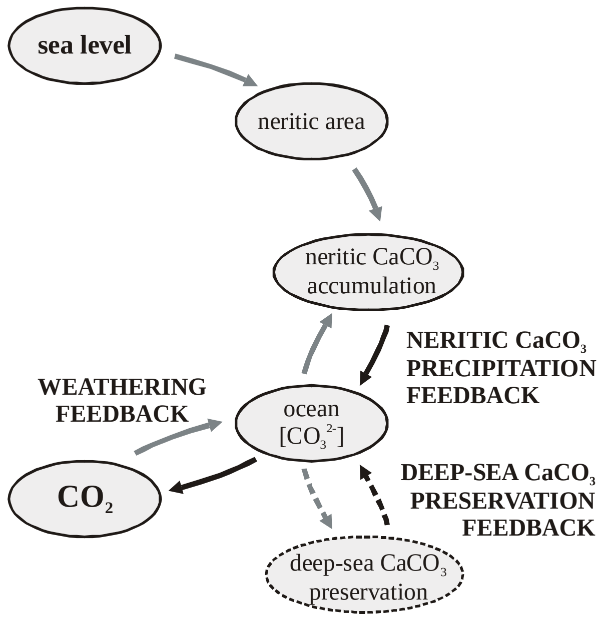

Ridgwell_Figure_04

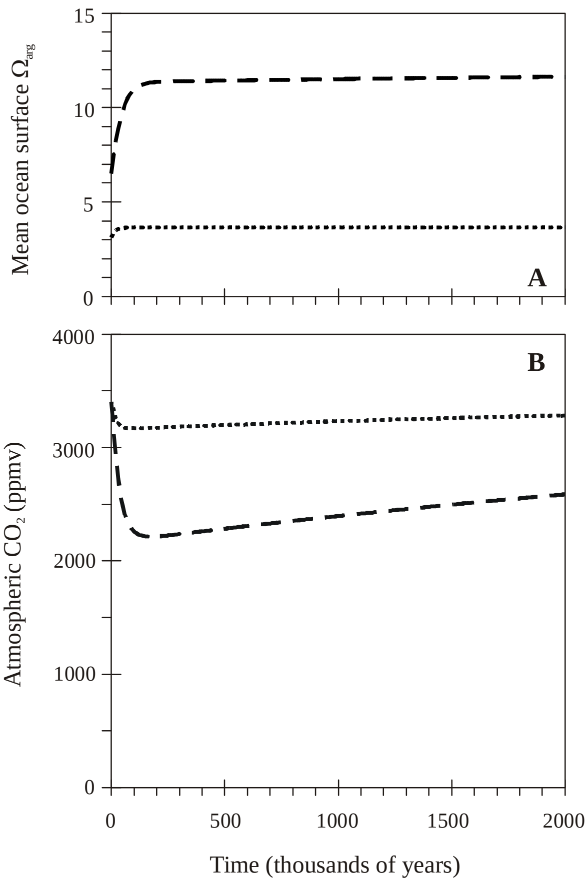

Ridgwell_Figure_05

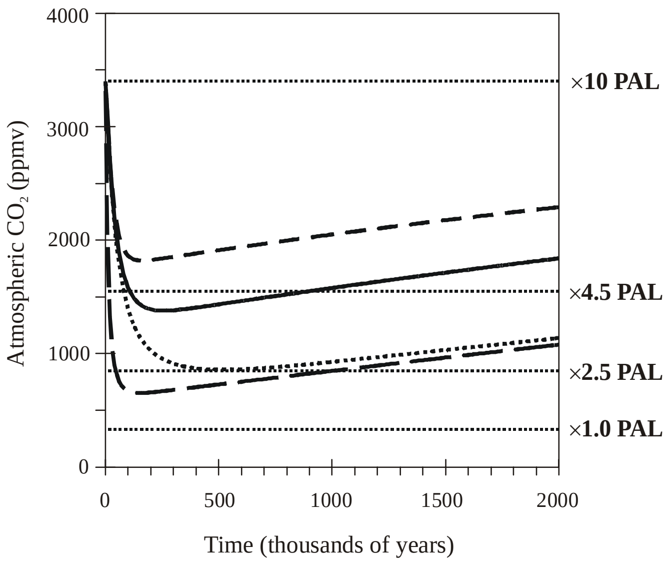

Ridgwell_Figure_06

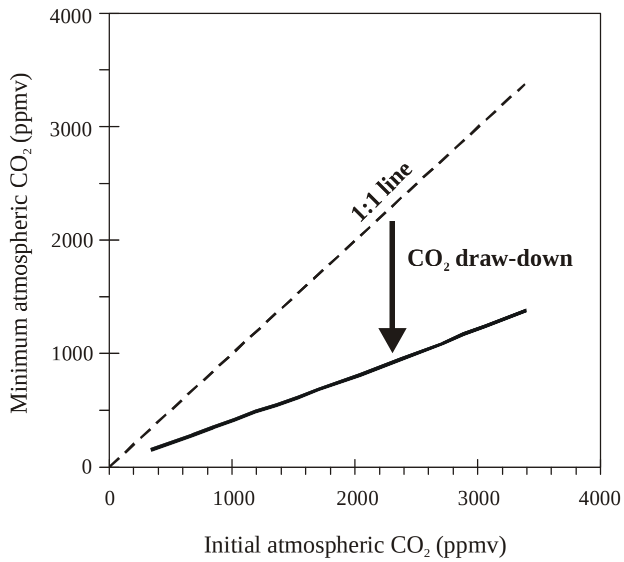

Ridgwell_Figure_07

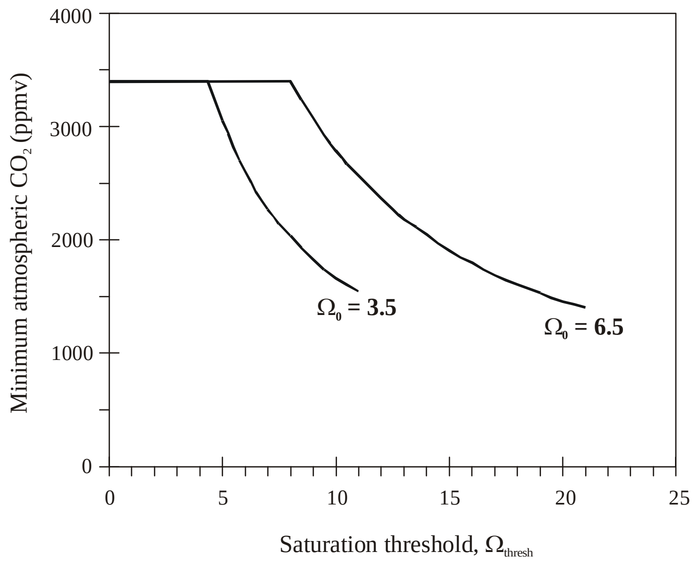

Ridgwell_Figure_08

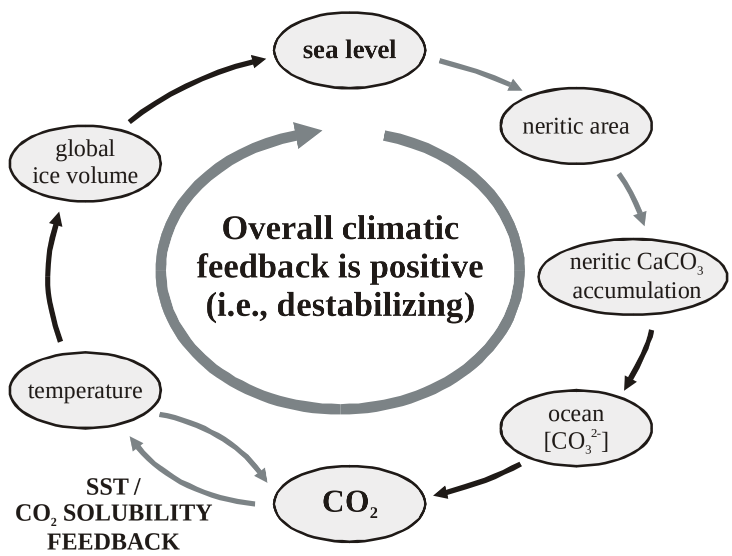

Ridgwell_Figure_09

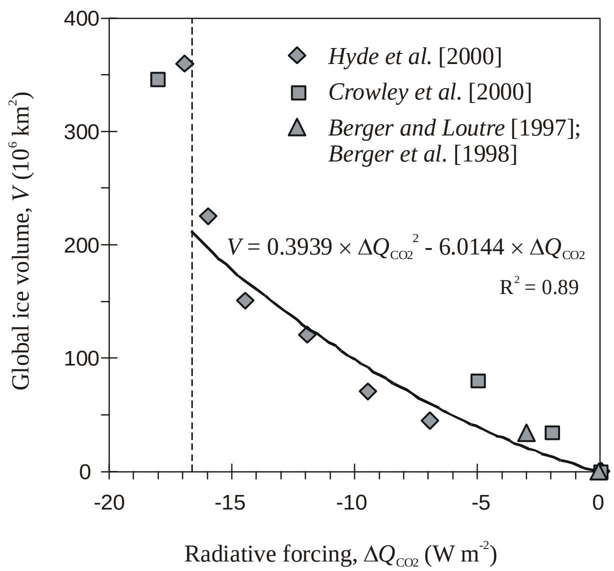

Ridgwell_Figure_10

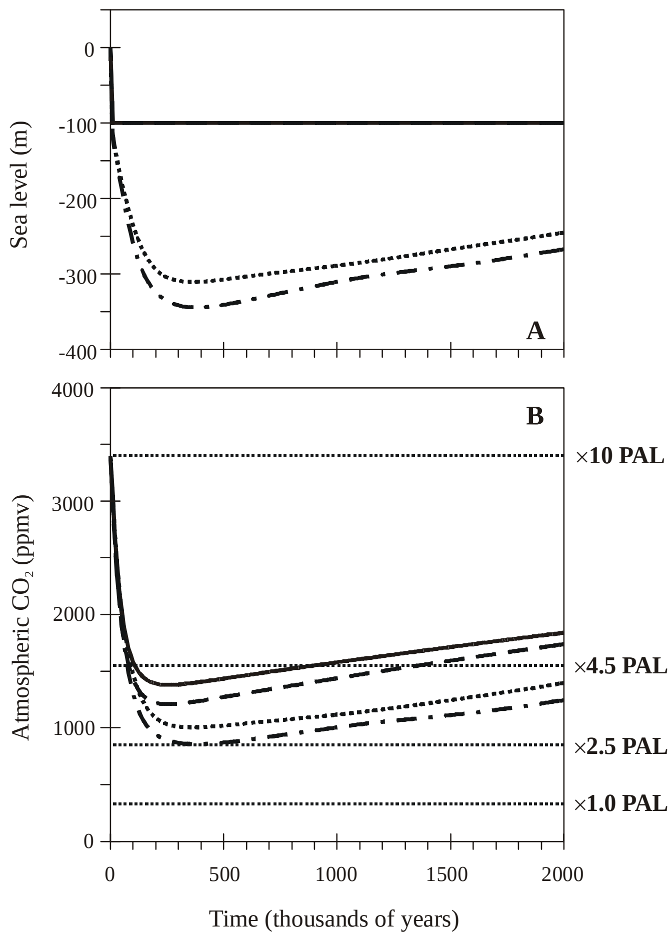

Ridgwell_Figure_11

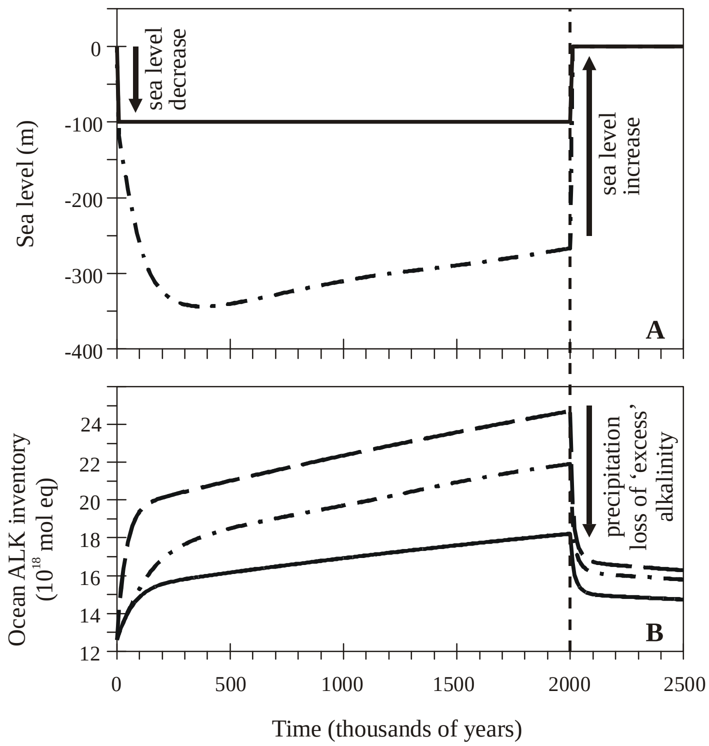

Ridgwell_Figure_12